

Distinct Columnar and Lamellar Liquid Crystalline Phases Formed by New Bolaamphiphiles with Linear and Branched Lateral Hydrocarbon Chains

Marko Prehm,^[a,b] Claudia Enders,^[a] Maryam Yahyae Anzahae,^[a] Benjamin Glettner,^[a] Ute Baumeister,^[b] and Carsten Tschierske*^[a]

Abstract: A universal building block for the convergent synthesis of a wide variety of different T-shaped ternary amphiphiles was developed and used for the synthesis of a series of new liquid-crystalline materials composed of a rigid biphenyl core with polar glycerol groups at both ends and linear or branched alkyl chains in a lateral position. In addition, compounds with bulky achiral (2,4,6-trimethylphenoxy, adamantane-1-carboxylate, benzoate) or chiral (menthyl or cholesteryl) substituents attached to the end of the lateral alkyl chain were also investigated. In all cases the lateral chains were connected to the aromatic core by an

ether linkage. The effect of the ether linking unit on mesophase stability and mesophase type is discussed with respect to conformational effects. The liquid-crystalline phases were investigated by polarizing microscopy, calorimetry, and X-ray diffraction of surface aligned samples. Upon enlarging the lateral chains a series of different polygonal cylinder phases was observed, which were replaced by lamellar phases and a non-cylinder hexago-

nal columnar phase by further increasing the size of these substituents. Remarkably, only pentagonal, hexagonal, and giant hexagonal cylinder phases could be observed, whereas mesophases composed of cylinders with a smaller number of sides are missing. No distinct chirality effects were observed for the menthyl- and cholesteryl-substituted compounds. However, the rodlike shape of the polycyclic cholesteryl core leads to a unique phase structure combining an organization of the alicyclic cholesteryl cores perpendicular to the layer planes and the aromatic biphenyl cores parallel to the layer planes.

Keywords: amphiphiles • liquid crystals • mesophases • self-assembly • supramolecular chemistry

Introduction

The design of new molecules forming novel types of liquid-crystalline (LC) phases^[1] is of contemporary interest for the fundamental understanding of soft-matter self-organization.^[2,3] Segregation of incompatible molecular segments into distinct regions is one of the fundamental driving forces

for the self-organization of amphiphilic molecules.^[4] Low-molecular-weight, dendritic or polymeric amphiphiles (e.g. block copolymers), composed of only two different molecular parts, usually change their organization depending on the volume fractions of the two incompatible parts. Thereby, with increasing volume fraction of one of the parts, starting from layer structures (smectic phases) for nearly equal volume fractions, the mesophase morphology changes at first to columnar and then to mesophases composed of spheroidal aggregates (see Figure 1).^[5–9] Additionally, bicontinuous cubic phases (Cub_v) and perforated layer structures were observed as intermediate phases at the transition from lamellar to columnar organization.^[5,7,8] However, the

[a] Dr. M. Prehm, Dipl.-Chem. C. Enders, M. Y. Anzahae, Dipl.-Chem. B. Glettner, Prof. Dr. C. Tschierske
Institute of Chemistry, Organic Chemistry
Martin-Luther-University Halle-Wittenberg
Kurt-Mothes-Str. 2, 06120 Halle (Germany)
Fax: (+49) 345-552-7346
E-mail: carsten.tschierske@chemie.uni-halle.de

[b] Dr. M. Prehm, Dr. U. Baumeister
Institute of Chemistry, Physical Chemistry
Martin-Luther-University Halle-Wittenberg
Mühlporfte, 06108 Halle (Germany)

Supporting information for this article is available on the WWW under <http://www.chemeurj.org/> or from the author. It contains additional figures (textures and X-ray diffraction patterns), tables with X-ray data, experimental procedures, and analytical data.



Figure 1. General phase sequence of conventional amphiphiles with respect to the increasing volume fraction of one of the incompatible parts.

number of possible structures that can be realized with these binary amphiphiles is limited mainly to these few morphologies.

Mesophase morphologies with higher levels of complexity can be achieved with polyphilic molecules,^[10] combining more than two incompatible units, as successfully demonstrated for low-molecular-weight T-shaped ternary amphiphiles.^[11–14] and ABC-triblock copolymers.^[5,15–17] A wide variety of different complex soft-matter superstructures was obtained for the bolaamphiphiles **An** (Figure 2).^[12a] Here, the

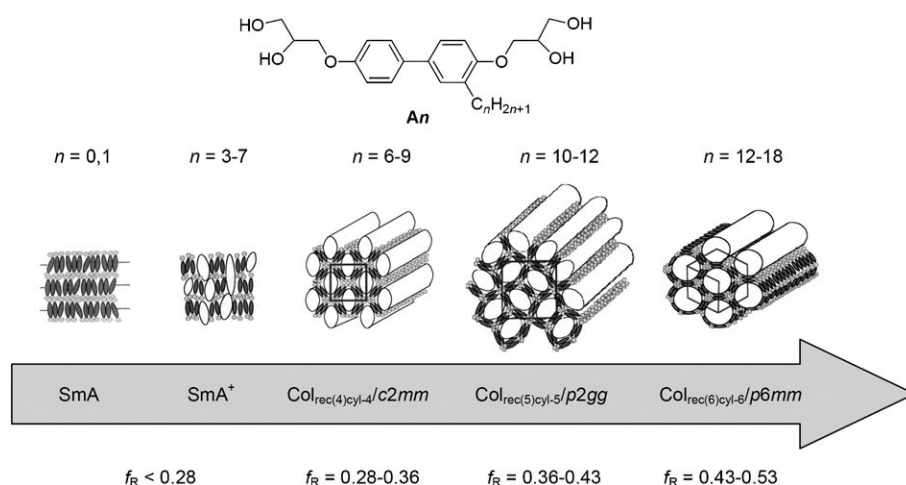


Figure 2. Dependence of the liquid-crystalline phases of the previously reported alkyl-substituted bolaamphiphilic tetraols **An**, on the length (n) and the volume fraction (f_R) of the lateral alkyl chain^[12a] (light gray = hydrogen-bonding networks of the terminal diol groups; white = microsegregated regions of the lateral chains; gray = rigid biphenyl units).

organization of the flexible nonpolar chains is in competition with the organization provided by the rigid biphenyl units and the polar hydrogen-bonding networks. As shown in Figure 2, elongation of the lateral alkyl chain of compounds **An** gives rise to a transition from smectic A phases (molecules are aligned, on average, perpendicular to the layer planes, SmA) to a series of columnar phases composed of cylinders with a polygonal cross section (rhombuses: Col_{rec}/c2mm; squares: Col_{squ}/p4mm; pentagons: Col_{rec}/p2gg, hexagons: Col_{hex}/p6mm).^[12a] In these columnar mesophases the fluid alkyl chains are organized within columns and the bolaamphiphilic units form cylinder shells framing these columns. Hence, the space required by the lateral chains with respect to the length of the bolaamphiphilic moieties determines the shape of the cylinders; the periodic packing of these cylinders gives rise to honeycomb-like arrays representing different types of 2D lattices.^[11,12a,14]

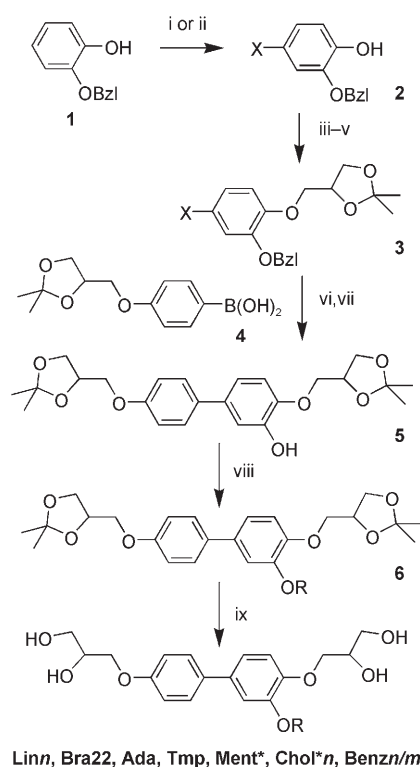
By using fluorinated lateral chains it was possible to further increase the size of the lateral substituents, which lead to giant cylinder structures built up by stretched hexagons with eight (8-hexagons) or even ten molecules (10-hexagons) in the circumference (Col_{rec}/c2mm phases) in which two or four sides are formed by end-to-end pairs of molecules.^[12b–d]

In the mesophase code used to describe these cylinder structures^[11] the type of the columnar phase is given first (Col_{hex}, Col_{rec}), followed by the shape of the cylinder cross section, given by a number in brackets, indicating the number of walls forming one cylinder (e.g., 6 means hexagons). The abbreviation “cyl” indicates the polygonal cylinder structure and the last numerical indicates the number of molecules in the circumference of each cylinder. This is important for the giant cylinder phases in which some cylinder walls are formed by end-to-end pairs. After the slash the plane group is given. For example, Col_{rec(6)cyl-8}/c2mm describes a stretched hexagonal cylinder phase in which each hexagonal cylinder has eight molecules in the circumference (8-hexagons) and the resulting plane group is c2mm (see Figure 12 in the Conclusions section).^[11]

Also a novel class of lamellar liquid-crystalline phases was found for these compounds with fluorinated lateral chains. In these lamellar phases the aromatic cores and the lateral chains are organized in distinct layers. In contrast to the smectic phases of classical rodlike LC molecules, in which the rodlike cores are arranged perpendicular to the layer planes or slightly tilted with respect to the layer normal, in these lamellar phases the rodlike cores of the bolaamphiphiles are completely disordered (Lam_{iso} phase) or aligned on average parallel to the layer planes (Lam_N and Lam_{Sm} phases).^[12b,c,13,18,19] In the lamellar nematic phase (Lam_N) the aromatic cores adopt a long-range orientational order in the layers and between adjacent layers there is an orientational correlation. Hence in this lamellar phase there is a nematic-like order in the aromatic sublayers and therefore this phase is assigned as lamellar nematic phase (Lam_N). Similarly, in the lamellar smectic phases (Lam_{Sm}) the rodlike cores adopt a smectic-like in-plane order.^[18]

In the series of compounds reported previously the lateral alkyl or perfluoroalkyl chains were attached directly to the aromatic core; this required lengthy syntheses and introduction of these substituents in one of the first steps of the synthesis.^[12a–c] However, the synthesis of molecules with longer and more complex lateral chains requires a more convergent synthetic strategy.

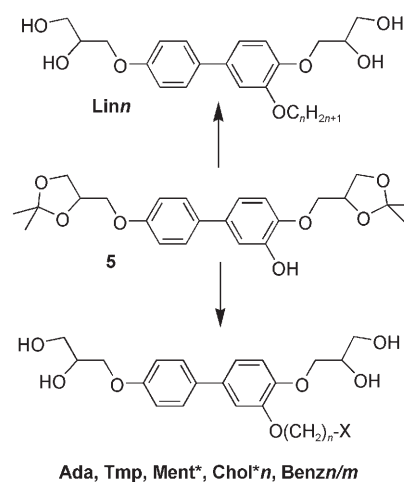
Herein we report a convergent methodology of synthesis for bolaamphiphiles in which the lateral chains were attached in one of the last synthetic steps (Scheme 1; compounds **1–6**). This was achieved with the hydroxyl-functionalized building block **5** (see Scheme 2), which can be alkylated with different halides or tosylates to yield a wide variety



Scheme 1. Synthesis of the compounds: Reagents and conditions: i) X = I: NaI, NaOCl, NaOH, MeOH, 0 °C, 1 h;^[22] ii) X = Br: Br₂/AcOH/CH₂Cl₂, 0 °C, 15 min;^[23] iii) BrCH₂CH=CH₂, K₂CO₃, CH₃CN, 80 °C, 6 h; iv) OsO₄, *N*-methylmorpholine-*N*-oxide, 20 °C, 48 h;^[24,25] v) 2,2-dimethoxypropane, pyridinium *p*-toluene sulfonate, 20 °C, 24 h; vi) [Pd(PPh₃)₄], NaHCO₃, glyme, H₂O, reflux, 6 h;^[20] vii) H₂, Pd/C, EtOAc, 40 °C, 12 h; viii) RX, K₂CO₃, DMF, Bu₄NI, 80 °C, 6 h; ix) 10% HCl, MeOH, reflux, 6 h; abbreviations of the compounds: **Linn**: compounds with linear alkoxy chains, *n* gives the number of carbon atoms in the lateral chain (*n* = 6–12, 14, 16, 18, 20, 22); **Bra22**: R = 2-decyldodec-1-yl; for **Ada**, **Tmp**, **Ment***, **Chol*n** and **Benzn/m**: R = (CH₂)_{*n*}X; **Ada**: X = adamantane-1-carbonyloxy, *n* = 11; **Tmp**: X = 2,4,6-trimethylphenoxy, *n* = 12; **Ment***: X = (1*R*,2*S*,5*S*)-menthyloxy, *n* = 12; **Chol*n**: X = cholest-5-en-3β-oxy, *n* = spacer length (*n* = 6, 11); **Benzn/m**: X = benzyloxy, *n* = spacer length (*n* = 6, 11) and *m* gives the number of dodecyloxy chains attached to the benzoyl group (*m* = 1: 4-dodecyloxy, *m* = 2: 3,4-didodecyloxy, *m* = 3: 3,4,5-tridodecyloxy).

of different molecular architectures. As a consequence of this synthetic strategy, all these compounds contain an additional ether linkage between aromatic core and lateral chain. The influence of this additional ether linkage on the mesomorphic properties was investigated first and then new series of bolaamphiphiles with extremely large and more complex lateral groups were synthesized (see Scheme 2).

With these molecules giant cylinder structures, as well as Lam_N and Lam_{Sm} phases, previously reported only for fluorinated molecules,^[12b,13] were obtained for alkyl-substituted T-shaped bolaamphiphiles if the size of the lateral chains was increased sufficiently. Compounds with extremely bulky lateral groups form a new noncylinder mode of organization in which the bolaamphiphilic cores are organized in columns that are surrounded by the lateral chains. A cholesteryl group in the lateral chain can act as a second distinct rigid



Scheme 2. T-shaped ternary amphiphiles under discussion and key building block (compound 5) used for the synthesis of these compounds; for the abbreviations of the compounds see the legend of Scheme 1.

core that leads to a unique new phase structure in which the aromatic cores are organized parallel to the layers as typical for Lam phases and the cholesteryl moieties form separate layers; these units are organized with their long axes perpendicular to the layers as in usual smectic phases (SmA phases).

Results and Discussion

Synthesis: Scheme 1 describes the general synthetic pathway used for all compounds. Accordingly, acetone-protected glycerol-substituted aryl halides **3** (X = Br, I) were coupled in Miyaura–Suzuki cross-coupling reactions^[20] with 4-(2,2-dimethyl-1,3-dioxolan-4-ylmethoxy)benzene boronic acid (**4**).^[12a] For the synthesis of the benzyloxy-substituted aryl halides **3**, 2-benzyloxyphenol^[14d,21] was halogenated in *para* position to the phenolic OH group by means of NaI/NaOCl/NaOH^[22] or Br₂/AcOH/CH₂Cl₂.^[23] The introduction of the terminal propane-2,3-diol groups was achieved by allylation followed by OsO₄-catalyzed dihydroxylation^[24,25] and these diol groups were protected as cyclic acetals before the coupling reaction was carried out. The benzyl protecting group was removed by catalytic hydrogenation to yield the OH functionalized bolaamphiphilic biphenyl derivative **5**, with acetone protected diol groups at both ends. Compound **5** was then used for the etherification reaction with appropriate alkyl bromides or tosylates. The *n*-alkyl bromides were commercially available, and the synthesis of the *ω*-functionalized halides and tosylates is described in the Supporting Information. All acetone-protected compounds **6** were purified by preparative centrifugal thin-layer chromatography with a Chromatotron (Harrison Research). In the final step the acetone protecting groups were removed by acidolytic cleavage. The obtained amphiphiles were purified by repeated crystallization from appropriate solvents and characterized by ¹H NMR, ¹³C NMR and elemental analysis. The purity was additional-

ly checked by TLC. The synthesis of compound **Lin 18** is reported in the Experimental Section as example, for all other compounds the procedures and analytical data are reported in the Supporting Information.

Mesomorphic properties

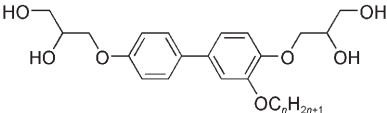
Polarized light optical microscopy, differential scanning calorimetry, and X-ray diffraction were used to determine the mode of self-assembly in the liquid-crystalline phases.

Compounds Lin n with linear chains—transition from smectic phases via cylinder phases to lamellar phases: The transition temperatures and corresponding enthalpy values of the *n*-alkoxy-substituted bolaamphiphiles **Lin n** are collated in Table 1. All compounds with short chains ($n=6-11$)^[26] have monotropic (metastable) liquid-crystalline phases, whereas those of the higher homologues are enantiotropic (thermodynamically stable). Increasing the length of the lateral chain gives rise to a transition from layer structures (SmA phases; $n=6-8$) to polygonal cylinder phases ($n > 8$) and fi-

nally for $n > 20$ to a Lam_{Sm} phase, in which the organization of the rodlike biphenyl cores is parallel to the layer planes.

SmA phases: In the SmA phases of compounds **Lin 6** and **Lin 8** the biphenyl cores should be aligned on average perpendicular to the layer planes and separated by layers formed by the hydrogen-bonding networks of the diol groups (SmA, Figure 2).^[27,28] The laterally attached alkyl chains are located between the biphenyl cores and disturb this organization due to their tendency to form separate compartments in which these flexible chains, which are incompatible with the aromatic cores, are localized. This leads to a reduction of the SmA–Iso phase-transition temperature by elongation of this chain from **Lin 6** to **Lin 8**. However, it seems that the relatively short chains^[26] of compounds **Lin 6–Lin 8** cannot fundamentally change the phase structure. In the case of compounds **Lin 9–Lin 22** with longer lateral chains, these chains are segregated into well-defined micro compartments that give rise to the formation of polygonal cylinder structures.

Table 1. Mesophases of compounds **Lin n** with nonbranched alkyl chains.^[a]



<i>n</i>	<i>T</i> [°C] ^[a] <i>ΔH</i> [kJ mol ⁻¹]	Phase	Lattice parameters [nm]			<i>f</i> _{OR} ^[b]	<i>n</i> _{cell} ^[c]	<i>n</i> _{wall} ^[d]
			<i>a</i>	<i>b</i>	<i>d</i>			
Lin 6	Cr 97 (SmA 84) Iso <i>33.1</i> <i>2.9</i>				<i>–</i> ^[e]	0.29		
Lin 8	Cr 100 (SmA 77) Iso <i>20.9</i> <i>1.2</i>				<i>–</i> ^[e]	0.35		
Lin 9	Cr 116 (Col _{rec(5)cyl-s} /p2gg 90) Iso <i>15.6</i> <i>3.8</i>		5.78	5.55		0.37	20.0	
Lin 10	Cr 112 (Col _{rec(5)cyl-s} /p2gg 100) Iso <i>29.0</i> <i>4.6</i>		5.65	5.32		0.39	18.1	
Lin 11	Cr 115 (Col _{hex(6)cyl-d} /p6mm 113) Iso <i>29.6</i> <i>5.0</i>		3.55			0.42	6.4	
Lin 12	Cr 101 Col _{hex(6)cyl-d} /p6mm 121 Iso <i>25.0</i> <i>6.4</i>		3.60			0.44	6.3	
Lin 14	Cr 92 Col _{hex(6)cyl-d} /p6mm 131 Iso <i>6.10</i> <i>7.5</i>		3.64			0.47	6.0	
Lin 16	Cr 65 Col _{hex(6)cyl-d} /p6mm 132 Iso <i>37.4</i> <i>7.3</i>		3.60			0.50	5.6	
Lin 18	Cr 78 Col _{rec(6)cyl-s} /c2mm 123 Col _{hex(6)cyl-d} /p6mm 126 Iso <i>19.1</i> <i>0.7</i> <i>5.1</i>		3.63 ^[f] 3.60 ^[g]	9.58 ^[g]		0.53	5.3 ^[f] 16.0 ^[g]	
Lin 20	Cr 77 Col _{rec(6)cyl-s} /c2mm 125 Iso <i>19.6</i> <i>6.8</i>		3.70	9.70		0.56	15.7	
Lin 22	Cr 93 Col _{rec(6)cyl-s} /c2mm 117 Lam _{Sm} 123 Iso <i>7.0</i> <i>1.0</i> <i>4.4</i>		3.86 ^[g]	9.64 ^[g]	3.64 ^[h]	0.58	15.5 ^[g]	

[a] Transition temperatures (*T* [°C]) and corresponding enthalpy values (*ΔH* [kJ mol⁻¹], lower lines, in italics) were taken from the second DSC heating scans (10 K min⁻¹); values in parenthesis indicate monotropic mesophases, in this case the enthalpy values were measured in the first cooling scan and the transition temperatures were determined by polarizing microscopy. Cr=crystalline phase, Iso=isotropic liquid phase, Col_{rec(6)cyl-s}/c2mm=centered rectangular columnar phase with c2mm plane group symmetry, representing a hexagonal honeycomb formed by stretched hexagonal cylinders with 8 molecules in the circumference (8-hexagons), Lam_{Sm}=lamellar smectic phase, the other phases are shown in Figure 2. [b] *f*_{OR}=volume fraction of the lateral chain, including the ether oxygen (calculated using crystal volume increments).^[30] [c] *n*_{cell}=number of molecules per unit cell, calculated according to $n_{\text{cell}} = V_{\text{cell}}/V_{\text{mol}}$ from the volume of the unit cell (*V*_{cell}) defined by the dimensions $a \times b \times 0.45$ nm for rectangular phases and $a^2 \times \sin(60^\circ) \times 0.45$ nm for hexagonal phases and the molecular volumes (*V*_{mol}) using crystal volume increments,^[30] considering the reduced packing density in the LC state (for more details of calculations, see Table S2). [d] *n*_{wall}=average number of molecules in the cross section of the cylinder walls=*n*_{cell} divided by the number of cylinder walls per unit cell. [e] Not determined due to rapid crystallization of the sample. [f] Value for the Col_{hex(6)cyl-d}/p6mm phase. [g] Values for the Col_{rec(6)cyl-s}/c2mm phase. [h] Value for the Lam_{Sm} phase.

Pentagonal cylinder phases: The typical textures and X-ray diffraction patterns of the polygonal cylinder phases, obtained for compounds **Lin 9–Lin 22**, are shown in Figures 3 and 4. In all cases the wide-angle scattering is diffuse (Figure 3b,e), which indicates the fluid character of these mesophases.^[29] The small angle scattering provides information about the lattice type and the lattice parameters. For compounds **Lin 9** and **Lin 10** the diffraction pattern can be indexed to a $p2gg$ lattice with parameters ($a=5.7\text{--}5.8\text{ nm}$, $b=5.3\text{--}5.5\text{ nm}$, see Table 1) ranging between 2.3 and 2.7 times the molecular lengths, measured between the ends of the two glycerol units in the most stretched conformation ($L=2.1\text{ nm}$). This is a typical range that is also observed for the pentagonal cylinder phases ($\text{Col}_{\text{rec}(5)\text{cyl-5}}/p2gg$) of the related n -alkyl derivatives **An** with $n=10\text{--}12$ ^[12a] and bolaamphiphiles with fluorinated lateral chains.^[12b] In these cylinder phases the aromatic cores are organized in pentagonal cylinder frames, the alkyl chains fill the interior of the cylinders, and the hydrogen-bonding networks running along the edges fuse these cylinders edge-to-edge and side-by-side,

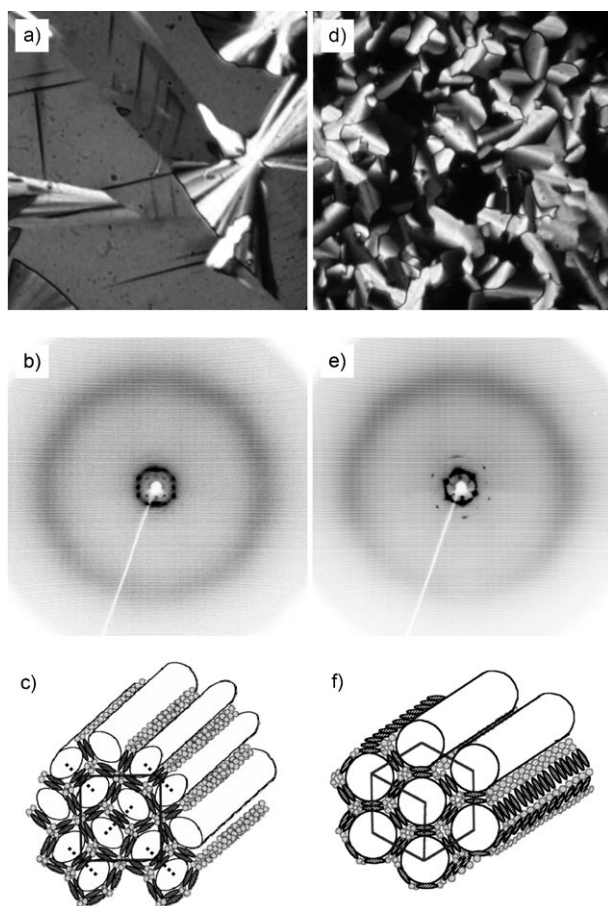


Figure 3. a),d) Textures, b),e) X-ray diffraction patterns of surface aligned samples, and c),f) models of self-assembled superstructures formed by compounds **Lin 9–Lin 12**. $\text{Col}_{\text{rec}(5)\text{cyl-5}}/p2gg$ phases of a) **Lin 9** at $T=85^\circ\text{C}$, b) **Lin 10** at $T=98^\circ\text{C}$, and c) model of the phase (the dotted lines indicate the cylinder pairs which adopt a herring bone-like packing on a $p2gg$ lattice); $\text{Col}_{\text{hex}(6)\text{cyl-6}}/p6mm$ phases d) **Lin 11** at $T=110^\circ\text{C}$, e) of **Lin 12** at $T=109^\circ\text{C}$, and f) model of the phase.

yielding a pentagonal honeycomb, as shown in Figure 3c. These pentagonal cylinders form pairs that organize in a herringbone pattern. Formation of cylinder pairs leads to units with enhanced symmetry, and for this reason the pentagonal symmetry is lost and replaced by the experimentally observed rectangular lattice with plane group $p2gg$ (see Figure 3c). Moreover, as regular pentagons cannot tile a plane, the individual cylinders do not have a regular pentagonal cross section, but instead these are non-regular pentagons in which not all side-length and angles are exactly the same. This slight deformation of the cylinders is possible in the fluid LC state and allows a tiling of space by (nonregular) pentagonal cylinders. The number of molecules per unit cell (n_{cell}) was calculated by dividing the unit cell volume by the molecular volume (determined by using crystal volume increments^[30] and considering the reduced packing density in the LC state, as described in the Supporting Information, see Table S2). The unit cell is defined by the lattice parameters and a height of $h=0.45\text{ nm}$, corresponding to the mean distance between the aliphatic chains and the aromatic cores (determined from the position of the maximum of the diffuse wide-angle scattering in the X-ray diffraction pattern). The number of molecules obtained in this way is between $n_{\text{cell}}=18$ and 20 (see Table 1 and Table S2). This number is completely in line with the proposed phase structure composed of four pentagonal cylinders per unit cell ($4\times 5=20$). The thickness of the cylinder walls is on average about two molecules ($n_{\text{wall}}=1.8\text{--}2.0$ ^[31]), which is a very typical value found for nearly all cylinder phases.^[11,12,32] Hence, the rectangular columnar phases of compounds **Lin 9** and **Lin 10** represent $\text{Col}_{\text{rec}(5)\text{cyl-5}}/p2gg$ phases composed of pentagonal cylinders in which each cylinder has five molecules in the circumference and the resulting plane group is $p2gg$.^[11]

Hexagonal cylinder phases: For the mesophases of compounds **Lin 11–Lin 16** with longer chains the textures and the X-ray diffraction patterns (Figure 4a,b) indicate hexagonal columnar phases ($a_{\text{hex}}=3.5$ to 3.6 nm). As typical for all hexagonal cylinder phases ($\text{Col}_{\text{hex}(6)\text{cyl-6}}/p6mm$ phases) the lattice parameter corresponds to $3^{1/2}$ of the molecular length L (see Table 1), indicating the size of the cylinder walls corresponds to the length of the bolaamphiphilic cores of the molecules in the most stretched conformation ($L=2.1\text{ nm}$). The number of molecules per unit cell is between $n_{\text{cell}}=5.3$ and 6.4, which is also in line with the proposed phase structure (one hexagonal cylinder per unit cell).^[32,33] Increasing the chain length further leads to other phase structures.

Giant cylinder phases: Compound **Lin 18** is especially interesting, as it shows a temperature-dependent transition from the $\text{Col}_{\text{hex}(6)\text{cyl-6}}/p6mm$ phase at high temperature to another mesophase at lower temperature. At the transition to the low-temperature phase, the texture changes completely, and the optically isotropic areas (dark areas in Figure 4a) become strongly birefringent (see Figure 4e). The diffuse wide-angle scattering in the diffraction pattern remains (see Figure S1c,d), but numerous new reflections occur in the

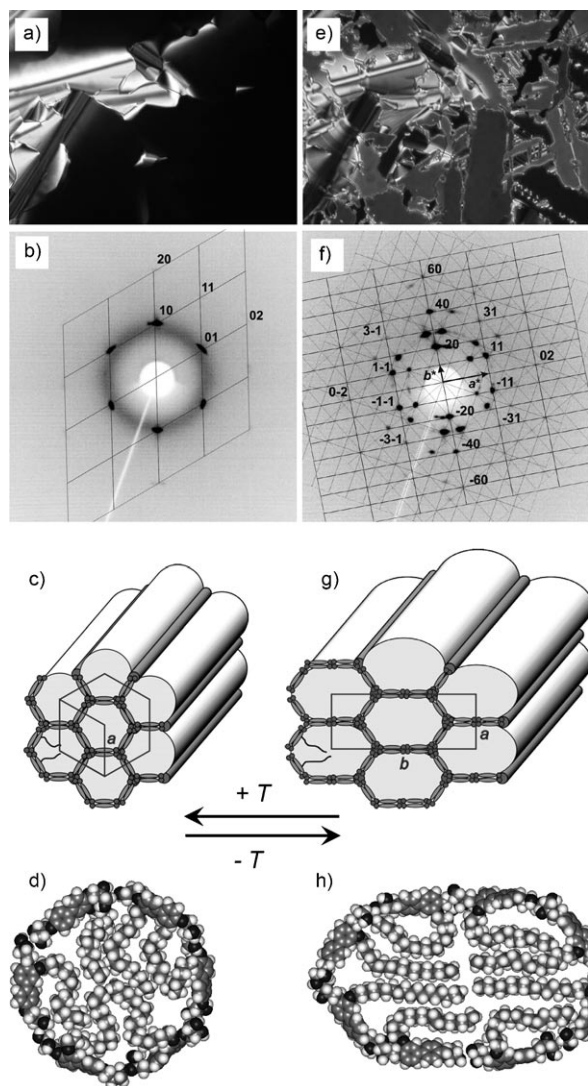


Figure 4. Mesophases of compound **Lin 18**: a)–d) $\text{Col}_{\text{hex}(6)\text{cyl-6}}/p6mm$ phase; a) texture at 125°C between crossed polarizers, b) X-ray diffraction pattern of an aligned sample at 124°C; c) model of the organization of the molecules in the mesophase; d) CPK model showing six molecules organized in the circumference of a 6-hexagon cylinder; e)–h) $\text{Col}_{\text{rec}(6)\text{cyl-8}}/c2mm$ phase; e) texture at 115°C, f) small-angle region of the X-ray diffraction pattern of an aligned sample at 90°C with indexation of one domain; g) model of the organization of the molecules in the mesophase; h) CPK model showing eight molecules organized in the circumference of a 8-hexagon cylinder; color versions of a) and e) are given in Figure S1a,b in the Supporting Information.

small-angle region (Figure 4f). Graphical analysis indicates a multidomain structure composed of three distinct domains. One of them is indexed in Figure 4f. All reflections correspond to $hk: h+k=2n$ ($h0: h=2n$ and $0k: k=2n$), which indicates a centered rectangular cell with the plane group $c2mm$ and lattice parameters $a=3.60$ nm and $b=9.58$ nm. The symmetry, the lattice parameters and the number of molecules per unit cell are in line with the model shown in Figure 4g. Accordingly, the structure is formed by cylinders with eight molecules in the circumference. As regular octagons cannot tile a plane without leaving void space, the oc-

tagons become deformed to stretched hexagons, in which the two longer sides are built up by end-to-end pairs of molecules (8-hexagons). The terminal diol groups segregate into columns of their own, located at the corners of these stretched hexagons and in the middle of the elongated cylinder walls. These columns of hydrogen-bonding networks interconnect the biphenyl cores, creating a honeycomb-like network in which the interior is filled by the lateral alkyl chains ($\text{Col}_{\text{rec}(6)\text{cyl-8}}/c2mm$ phase, see Figure 4g). The calculated number of $n_{\text{cell}}=16$ molecules per unit cell (see Table 1) is in good agreement with this model (16 molecules are required by two cylinders with 8 molecules in the perimeter) and indicates that also in this case each of the cylinder walls is formed by on average about two molecules in the diameter. This type of giant cylinder phase was previously observed only for few bolaamphiphiles with semiperfluorinated lateral chains^[12b,32] and is reported herein the first time for a non-fluorinated molecule.^[34]

The observed replacement of the regular hexagonal cylinders (6-hexagons) by larger stretched hexagonal cylinders upon elongation of the lateral chain from **Lin 16** to **Lin 20** can easily be understood. Because longer chains cannot fit into the limited space available within the 6-hexagons, elongation of these chains leads to an expansion of these cylinders to 8-hexagons. However, the fact that for compound **Lin 18** the 6-hexagon cylinder phase occurs at higher temperature than the 8-hexagon cylinder phase is surprising. As the alkyl chains have a larger thermal expansion coefficient compared to the glycerol units,^[35] it could be expected that with increasing temperature the columns inside the cylinders should expand most. This should favor the larger 8-hexagon cylinders at higher temperature. The unexpected phase sequence observed for **Lin 18**, in which the larger cylinder structure occurs at lower temperature, can be explained on the basis of the temperature dependence of the conformation of the alkyl chains. At higher temperature the alkyl chains are quite flexible and the comparatively long C_{18} alkyl chains can easily fill the hexagonal cylinders by adopting nonlinear conformations (Figure 4d). By reducing the temperature the flexibility of these chains is reduced and, hence, the chains cannot be accommodated in the small cylinders of the $p6mm$ phase. In the stretched hexagonal cylinders of the $c2mm$ phase with eight molecules in the circumference more chains can be organized parallel to each other and in these cylinders less chain deformation is required (see Figure 4h). This is thought to be a main effect favoring the larger cylinders at lower temperature.^[36,37]

Transition from giant cylinder phases to Lam_{sm} phase: Compound **Lin 20** shows the $\text{Col}_{\text{rec}(6)\text{cyl-8}}/c2mm$ phase ($a=3.70$ nm and $b=9.70$ nm) in the whole temperature range, whereas for compound **Lin 22** again two LC phases were detected. The high-temperature phase forms a spherulitic texture as shown in Figure 5a. Upon cooling, at $T=117^\circ\text{C}$, a strong change of the birefringence color can be seen and the texture becomes broken (Figure 5e). In the X-ray diffraction pattern of the high-temperature mesophase (see Figure 5b)

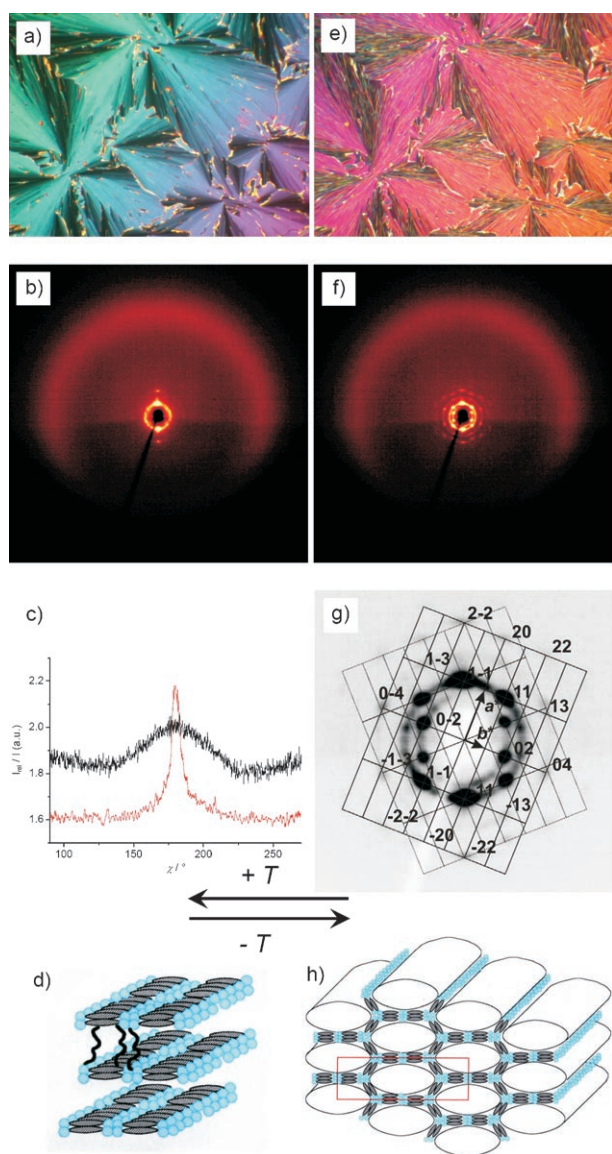


Figure 5. Mesophases of compound **Lin22**: a)–d) Lam_{Sm} phase; a) texture at 120°C between crossed polarizers, b) X-ray diffraction pattern of an aligned sample at 119°C; c) distribution of the wide-angle scattering along χ (black line) with maxima at 180° [$I_{\text{rel}} = I(119^\circ\text{C})/I(128^\circ\text{C}, \text{Iso})$] in comparison with the χ position of the layer reflections (red line); d) model showing the organization of the molecules; e)–h) $\text{Col}_{\text{rec}(6)\text{cyl-8}/c2mm}$ phase; e) texture at 110°C, f) X-ray diffraction pattern of an aligned sample at 105°C (wide-angle region); g) small angle region with indexation of one domain; h) model showing the organization of the molecules.

only a layer reflection with its second order, corresponding to $d = 3.64$ nm, can be seen on the meridian, indicating a mesophase with layer structure. The diffuse wide-angle scattering around $2\theta = 19.6^\circ$ ($d = 0.45$ nm) has a ringlike shape with a maximum on the meridian (see Figure 5b,c). Accordingly, this mesophase is a lamellar phase (Lam) composed of alternating aromatic and aliphatic layers. In this mesophase the aromatic cores and also significant parts of the alkyl chains should be organized predominately parallel to the layer planes.^[18] The optical appearance of this mesophase is

characterized by a spherulitic texture that is typical for LC phases with 2D periodicity. This suggests that beside the layer periodicity there is an additional periodicity between the hydrogen-bonding networks in the layers formed by the bolaamphiphilic cores (see Figure 5d).^[13,18,38] However, this additional periodicity is not evident in the X-ray diffraction pattern and therefore it is assumed that there is no long-range positional correlation of the in-plane periodicity between the hydrogen-bonding networks in adjacent layers. In this case the reflections, caused by the in-plane periodicity, should be smeared out to streaks parallel to the meridian and, due to the relatively small electron density modulation between aromatic cores and glycerol units,^[39] the intensity of these diffuse scatterings is apparently too small to be detected. This type of lamellar phases with a long-range orientational correlation (biphenyl cores are aligned parallel in adjacent layers) but only short-range positional correlation between the layers is assigned as Lam_{Sm} .^[18]

The diffraction pattern completely changes at the transition to the low-temperature phase (see Figure 5f,g). This pattern can be indexed to a centered rectangular $c2mm$ lattice with $a = 3.86$ nm and $b = 9.64$ nm, indicating a $\text{Col}_{\text{rec}(6)\text{cyl-8}/c2mm}$ giant cylinder phase (see Figure 5h). This is in line with the fact that reduction of temperature reduces the space required by the alkyl chains and this allows the organization of the molecules in a honeycomb cylinder structure instead of an organization in layers.

Hence, in the series of alkoxy-substituted bolaamphiphiles there is a transition from SmA phases to pentagonal and hexagonal cylinder structures, which are replaced by stretched giant hexagonal cylinders with eight molecules in the circumference, followed by a lamellar mesophase (Lam_{Sm}) upon further increasing the chain length. This phase sequence is the same as observed for compounds with fluorinated segments^[12b] and this indicates that fluorination is not required for the design of these mesophases. All these mesophases can also be obtained with simple alkyl derivatives if the chain length is increased sufficiently.

Comparison of lateral alkyl and alkoxy chains: In Figure 6 the new compounds **Lin** with lateral n -alkoxy groups are compared with related compounds **An** reported previously, which have directly attached n -alkyl chains.^[12a] The phase sequence in both homologous series is very similar, but the $\text{Col}_{\text{rec}(4)\text{cyl-4}/c2mm}$ phase formed by four-sided cylinders with a rhombic cross section, which was observed over a rather broad range of chain length for the alkyl-substituted compounds without an ether linkage^[12a,b] (**An** with $n = 6$ – 9 , see Figures 2 and 6) is completely suppressed in the series of compounds **Lin**. In this series the pentagonal cylinder phase is the smallest type of polygonal cylinder phases. Moreover, the distinct phase types are slightly shifted to shorter alkyl chain length for compounds **Lin**, indicating that the additional ether oxygen atom should also contribute to the overall space filling within the polygonal cylinders (therefore, the volume fractions of the lateral chains f_{OR} in Tables 1 and 2 were calculated including these ether oxygen

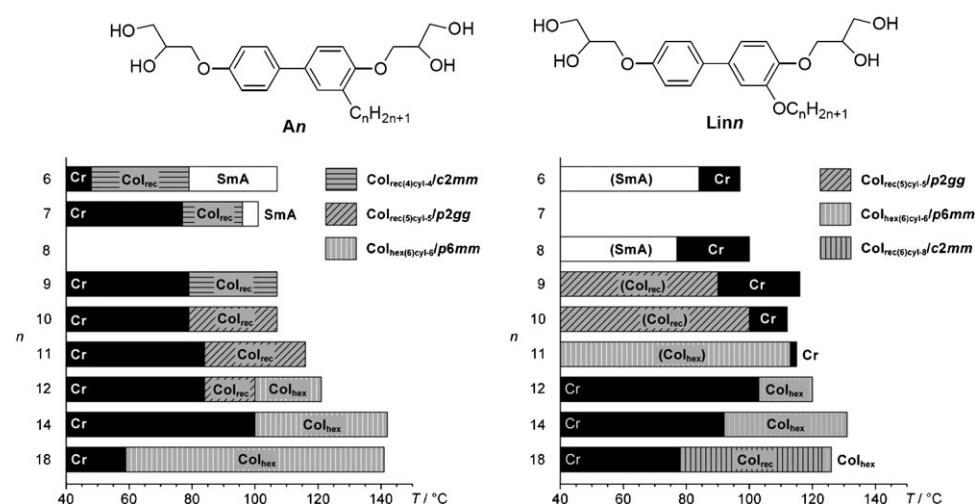


Figure 6. Comparison of the LC phases of alkyl-substituted (**An**)^[12a] and related alkoxy-substituted bolaamphiphiles (**Linn**) with the same number of C-atoms (n) in the lateral chain; monotropic mesophases in brackets; for the abbreviations of the mesophases, see Table 1 and Figure 2.

atoms).^[40] The comparison in Figure 6 also shows that the stabilities of the LC phases (LC-to-Iso transition temperatures) of the n -alkoxy-substituted compounds **Linn** are slightly lower than those of related n -alkyl-substituted bo-

laamphiphiles **An**. In addition, in most cases the melting points of the alkoxy-substituted compounds are higher, so that in general enantiotropic meso-

phases and broader mesomorphic regions were found for the alkyl-substituted compounds **An**. This mesophase destabilizing effect of replacing the alkyl by alkoxy groups in a lateral position at an aromatic rodlike core is completely reverse to its effect in terminal position, for which replacing alkyl groups by alkoxy groups always gives rise to mesophase stabilization if the rodlike unit is an aromatic system.^[1] The higher flexibility of the Ar-CH₂ linking unit compared to the Ar-O linking unit (different rotational barriers)^[41,42] should be mainly responsible for these effects. In terminal position the more rigid alkoxy groups favor the parallel alignment of the rodlike cores, which stabilizes LC phases. However, in lateral position the reduced flexibility makes the packing of these chains more difficult. The reduced flexibility should also be responsible for the missing of small cylinder structures composed of only four walls, as for example, the rhombic cylinders, seen for the Col_{rec(4)cyl-4/c2mm} phase of the alkyl-substituted compounds **An** ($n=6-9$, see Figures 2 and 6). As the orientation of the lateral chains with respect to the biphenyl core is more restricted for the alkoxy-substituted compounds it is more difficult for these chains to fill the space in these small cylinders efficiently.

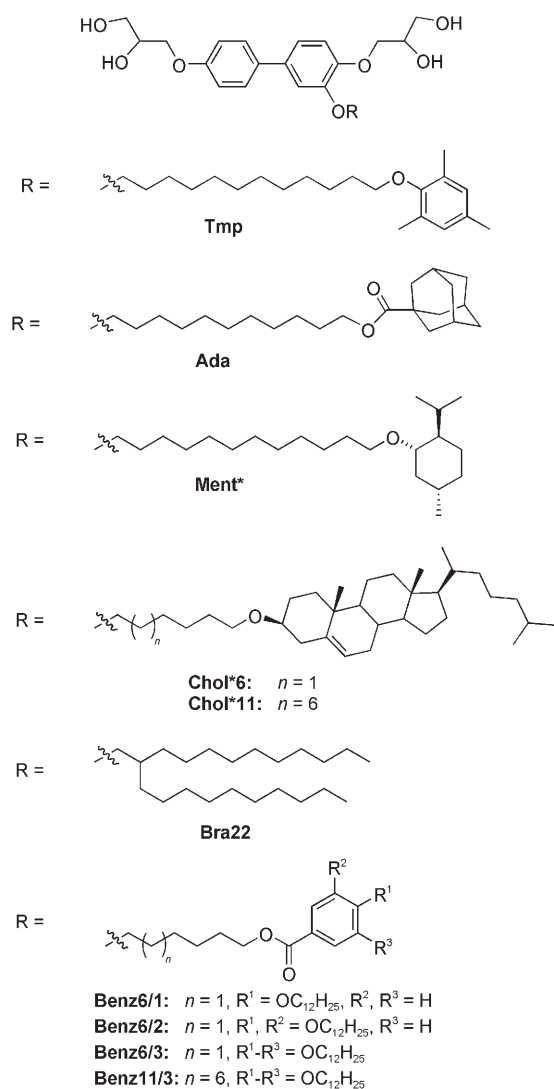
Compounds with bulky end groups:

The convergent synthetic strategy allows not only the preparation of simple n -alkoxy derivatives, but also the introduction of branched and other more complex lateral chains, as shown in Scheme 3 and in Table 2. Only a monotropic hexagonal columnar phase was observed for compound **Tmp** with a 2,4,6-trime-

Table 2. Mesophases of the bolaamphiphiles with bulky lateral chains.

	Total no of C+O atoms in R	T [°C] ^[a]		Lattice parameters [nm]			f_{OR}	n_{cell}	n_{wall}
		ΔH [kJ mol ⁻¹]	a	b	d				
Tmp	22	Cr 108 (Col _{hex(6)cyl-6/p6mm} 93) Iso	3.51			0.55	4.8	1.6	
		57.5 4.9							
Ada	24	Cr 62 Col _{hex(6)cyl-6/p6mm} 74 Iso	3.53			0.56	4.7	1.6	
		12.7 4.0							
Ment*	23	Cr 75 Col _{rec(6)cyl-8/c2mm} 103 Iso	3.73	9.52		0.58	14.8	1.9	
		16.6 5.5							
Chol*6	34	Cr 152 (Lam' _{Iso} 141) Iso			– ^[b]	0.66			
		49.6 1.1							
Chol*11	39	Cr 120 Lam' 136 Lam' _{Iso} 140 Iso			5.02 ^[c] 4.46 ^[d]	0.69			
		21.8 3.3 1.7							
Bra22	22	Cr 70 Lam _{Sm} 105 Iso		2.72		0.58			
		20.3 5.7							
Benz6/1	28	Cr 103 (M1 65 Lam _{Sm} 81) Iso		4.04		0.60			
		21.1 1.4 2.8							
Benz6/2	41	Cr 113 (Lam _N 102) Iso		4.70		0.69			
		76.3 3.1							
Benz6/3	54	Cr 104 Col _{hex} 121 Iso	4.95			0.75	11.6 ^[e]		
		69.7 2.0							
Benz11/3	59	Cr 84 Lam _N 103 Iso		5.25		0.77			
		48.9 5.3							

[a] Transition temperatures (T [°C]) and corresponding enthalpy values (ΔH [kJ mol⁻¹], lower lines, in italics) were taken from the second DSC heating scans (10 K min⁻¹); abbreviations: Lam_{Iso} = lamellar isotropic phase, composed of disordered sublayers of the bolaamphiphilic cores and the aliphatic lateral chains, Lam_N = lamellar nematic phase, in which the bolaamphiphilic cores are organized with their long axes parallel to the layer planes and adopt a long-range orientational order within these layers, the sublayers of the alkyl chains are disordered, Lam' and Lam'_{Iso} describe special types of Lam phases where biphenyl cores and cholesteryl units are organized in separate sublayers and the cholesteryl units adopt an organization on average perpendicular to the layer planes; Col_{hex} = non-cylinder hexagonal columnar phase; for the other abbreviations see Figure 2 and Table 1. [b] Not determined due to rapid crystallization. [c] Value for the Lam'_{Iso} phase. [d] Value for the Lam' phase. [e] In this case the volume of the unit cell was calculated by assuming a height of $h=1.8$ nm corresponding to the length of **Benz11/3** measured between the termini of the diol groups and assuming a most compact conformation of the glycerol groups.



Scheme 3. Structures of the bolaamphiphiles with bulky end-groups and branched lateral chains.

thylphenoxy group attached to the end of the lateral alkoxy chain (Figures S2a and S3). The lattice parameter $a_{\text{hex}} = 3.51 \text{ nm}$ is in the range expected for the hexagonal honeycomb structure ($\text{Col}_{\text{hex}(6)\text{cyl-}6}/p6mm$ phase). A hexagonal columnar phase was also found for the adamantane derivative **Ada** (Figures S2b and S4), whereas the menthol derivative **Ment***, with the largest number of atoms in the lateral chain, has a $\text{Col}_{\text{rec}(6)\text{cyl-}8}/c2mm$ phase ($a = 3.73 \text{ nm}$, $b = 9.52 \text{ nm}$, see Figure 7 and Figure S5 in the Supporting Information) composed of stretched hexagonal cylinders containing eight molecules in the circumference (see Figure 5h). This indicates that quite bulky units can be attached to the ends of the lateral chains of these compounds to produce structures in which these units can be accommodated in the interior of honeycomb cylinder frameworks with different shapes. This shows that it should in principle also be possible to attach

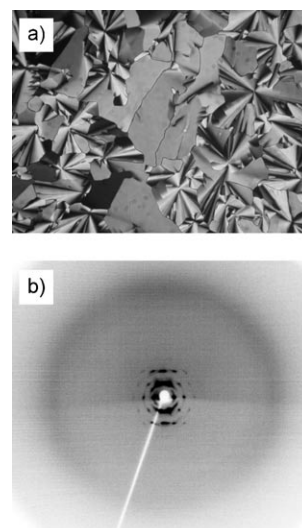


Figure 7. Compound **Ment***: a) texture of the $\text{Col}_{\text{rec}(6)\text{cyl-}8}/c2mm$ phase at 100°C (for a color version see Figure S5 in the Supporting Information); b) XRD pattern of an aligned sample at 95°C .

functional units to the ends of these chains, which can induce useful properties to these nanostructured systems.^[43]

A remarkable feature of the Col_{hex} phases of compounds **Tmp** and **Ada** is the relatively small number of molecules in the unit cell ($n_{\text{cell}} = 4.7\text{--}4.8$), which indicates a thickness of the cylinder walls of only 1.6 molecules on average.^[31] In Figure 8 the dependence of a_{hex} and n_{cell} on the volume fraction of the lateral chain (f_{OR}) is shown graphically for all compounds with Col_{hex} phases. Although a_{hex} is nearly independent of f_{OR} (the deviation of a_{hex} is due to limited accuracy of measurements and is about $\pm 0.05 \text{ nm}$, and because these parameters were determined at different temperatures) there is a clear decrease of n_{cell} , that is, the number of molecules organized in the cylinder walls decreases by enlarging the lateral substituent from $n_{\text{wall}} = 2.1$ for **Lin11** to $n_{\text{wall}} = 1.6$ for **Ada**. This indicates that increasing volume of

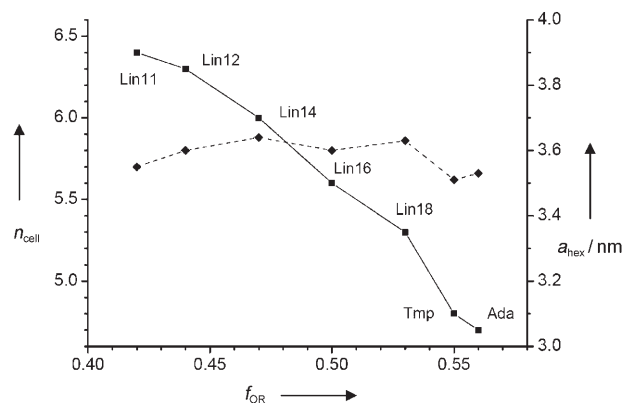


Figure 8. Dependence of the hexagonal lattice parameter a_{hex} (dashed line) and the number of molecules in a hexagonal unit cell (n_{cell} , solid line) on the volume fraction of the lateral chain (f_{OR}), as seen for the $\text{Col}_{\text{hex}(6)\text{cyl-}6}/p6mm$ phases of compounds **Lin11–Lin18**, **Tmp**, and **Ada**.

the lateral chain leads to an expansion of the lipophilic columns inside the hexagonal honeycombs. As the cross-section area available for the lateral chains inside the hexagonal cylinders is limited by the length of the bolaamphiphilic cores, the hexagonal lattice parameter increases only slightly upon enlarging the lateral chains. Hence, expansion of the lipophilic columns has to take place mainly along the column long axis. Due to this expansion the number of molecules in the cross section of the cylinder walls is reduced within certain limits. Therefore, n_{cell} and n_{wall} decrease with increasing size of the lateral substituent and temperature. This was observed for all polygonal cylinder phases and in all series of T-shaped bolaamphiphiles.^[11,12] As the cylinder walls become thinner these walls become also less stable and finally burst by giving way to other phase structures. The transition to 8-hexagons is often observed for hexagonal cylinder phases. It is also interesting to note that for molecules with linear alkyl chains (**Lin 11–Lin 18**) this transition already takes place at $f_{\text{OR}}=0.53$, whereas compounds **Tmp** and **Ada** with shorter chains and bulky end groups are a bit more robust and require $f_{\text{OR}} > 0.56$.

Effects of chirality: All the reported bolaamphiphiles contain two stereogenic centers in the glycerol units. Therefore, these compounds actually represent mixtures of diastereomers in their racemic forms. Herein attention is focused on molecules with additional stereogenic centers located in the functional groups attached to the ends of an aliphatic spacer unit.^[44] For the menthyl derivative **Ment*** the same type of $\text{Col}_{\text{rec}(6)\text{cyl-}8}/c2mm$ phase composed of giant hexagonal cylinders as previously observed for the linear compounds **Lin 18–Lin 22** was found. No special effects of the chirality on the phase structure, as for example, change of the phase symmetry or any hints on the induction of a helical superstructure,^[45] as common in other LC phases formed by chiral molecules, could be detected. Also for the compounds **Chol*n**, with cholesteryl groups in the lateral chain, no effect of chirality on the phase structure was observed. It seems that the hydrogen-bonding networks provide quite robust structures that cannot easily be modified by the relatively weak chirality effects in the lipophilic lateral chains. Nevertheless, the mesophases of compounds **Chol*n** are of interest from another point of view, as in these compounds two distinct rodlike units, the aromatic biphenyl core and a polyalicyclic core are combined in a competitive manner.

Effects of rodlike units in the lateral chain: The textures of the mesophases of compounds **Chol*6** and **Chol*11** with laterally attached cholesteryl units indicate the formation of lamellar phases (see Figure 9a). Compound **Chol*6** with a relatively short C_6 spacer shows only a monotropic uniaxial LC phase with a fanlike texture as typical for SmA and Lam_{iso} phases.^[18] Compound **Chol*11** with a much longer C_{11} spacer forms two different enantiotropic LC phases. The high-temperature mesophase shows a texture which is identical to that observed for **Chol*6**, characterized by regions with fanlike texture and regions that appear completely

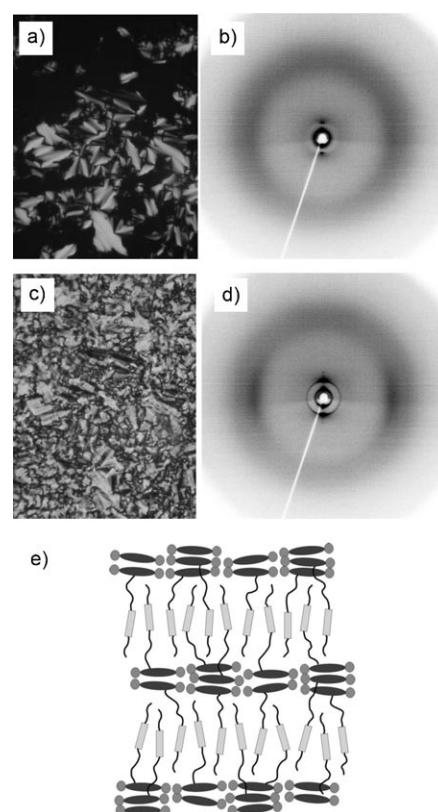


Figure 9. Compound **Chol*11**: a) texture of the Lam'_{iso} phase at 138°C; b) XRD pattern of an aligned sample at 136°C; c) texture of the Lam' phase at 130°C; d) XRD pattern of an aligned sample at 125°C; e) model showing the proposed organization of the molecules in the Lam' phase; color versions of a) and c) are shown in Figure S6 in the Supporting Information.

dark (see Figure 9a), which represent homeotropically aligned areas of a uniaxial lamellar phase. X-ray diffraction confirms a lamellar phase, characterized by layer reflections of the first- and second-order, corresponding to a layer distance of $d=5.02$ nm (Figure 9b). The wide-angle scattering is diffuse, which confirms the LC nature of this mesophase. For a surface-aligned sample the wide-angle scattering has a ring-like shape. Remarkably, weak, but distinct, maxima of the diffuse scattering corresponding to $d=0.54$ nm are located on the equator. They may be assigned to the mean distance between the cholesteryl units. In this case, the polycyclic cores of the cholesteryl units should adopt a preferred direction on average perpendicular to the layer planes as in conventional SmA phases and they are assumed to be segregated from the aliphatic segments (spacers and end chains at the cholesteryl groups) as well as from the bolaamphiphilic biphenyl cores. Hence, the lateral chains are completely intercalated, so that the rigid alicyclic cores of the cholesteryl units are located side by side and the spacer units and C_8 end chains of the cholesteryl unit are mixed and form common aliphatic sublayers, as shown schematically in Figure 9e for the more ordered low-temperature phase. However, in this high-temperature phase the orientational order is

not very high. The sublayers of the aliphatics and the bolaamphiphiles are nearly completely disordered as indicated by the ring-like shape of the diffuse scattering with the maximum at $d=0.46$ nm (Figure 9b). This phase is assigned as Lam'_{iso} .

At the transition to the low-temperature phase at 136°C a significant change of the texture as well as of the X-ray diffraction pattern is seen. In the texture of the lamellar low-temperature phase the homeotropically aligned regions, seen in Figure 9a, become birefringent (Figure 9c), indicating a transition to an optically biaxial mesophase (also after shearing, the sample remains birefringent and no pseudoisotropic areas can be detected). In the diffraction pattern the position of the layer reflection changes, that is, the layer distance is reduced to $d=4.46$ nm. The distinct maxima of the diffuse wide-angle scattering on the equator (at $d=0.54$ nm) become much stronger and less diffuse (Figure 9d). This indicates that the rigid polycyclic parts of the cholesteryl units retain an organization perpendicular to the layer planes, but the order parameter of these units is significantly increased in comparison to the high-temperature phase. An additional weaker maximum of the diffuse scattering is positioned on the meridian at $d=0.46$ nm, which is a typical feature of Lam phases.^[18] As the low-temperature phase is optically biaxial and a uniformly tilted organization as well as a mesophase with 2D lattice (columnar mesophase) is unlikely, judging from the diffraction pattern, it is thought that the phase transition is due to the inset of orientational long-range order within the sublayers of the bolaamphiphilic cores. This requires an arrangement of the biphenyl cores on average parallel to the layer planes as in Lam_N and Lam_Sm phases. As Lam_Sm and Lam_N phases cannot clearly be distinguished on the basis of X-ray diffraction patterns (in both cases only the layer reflections can be detected) and also textural observations do not allow an unambiguous distinction of these two phase types in this case, this low-temperature mesophase is tentatively assigned as Lam' . The birefringent texture developing in the homeotropically aligned regions (see Figure 9c) is not a schlieren texture as typical for Lam_N phases. Therefore, it is more likely that the low-temperature phase is related to the noncorrelated Lam_Sm phases with a periodicity within the layers, but with no long-range positional correlation between the layers. In any case, the mesophases of compounds **Chol****n* are unique, as the two different rodlike segments, the biphenyl units, and the rigid cycloaliphatic parts of the cholesteryl moieties are incompatible and organize into distinct sublayers (see Figure 9e). Moreover, the orientation of the two distinct types of rodlike units is different in the distinct sublayers. Whereas the biphenyl units are disordered (Lam'_{iso} phase) or organized with their long axes parallel to the layer planes (Lam' phase), the rigid parts of the cholesteryl units are organized on average perpendicular to the layers as in conventional SmA-type smectic phases. Hence, the Lam' phase is a triply segregated fluid smectic phase representing a hybrid structure composed of conventional SmA layers and Lam_N or Lam_Sm layers. This is a new LC phase structure that com-

bins two completely different types of lamellar organizations in one structure. There is an analogy to smectic phases of some combined LC main-chain/side-chain polymers^[46] with cholesteryl pedant groups. An intercalated layer morphology with the pedants oriented perpendicular to the backbones was also observed for these polymers.^[47] Other combined LC polymers with aromatic pedants form nematic phases where these pedants align parallel to the polymer backbone. Exclusively nematic phases, in which the distinct rodlike cores are mixed, have also been observed for all previously reported low-molecular-weight T-shaped dimesogens.^[48,49] It seems that in low-molecular-weight systems not only the incompatibility of the two distinct rigid units,^[50] but also the incompatibility of the groups attached to their ends (diol groups at the biphenyls and alkyl chains at the polyalicyclics) contribute to the formation of distinct sublayers comprising different rodlike units.

Effects of branching of the lateral chain: The X-ray diffraction pattern of the mesophase of compound **Bra22** with a branched lateral chain is characterized by a layer reflection, corresponding to $d=2.72$ nm in the small angle region (Figure S7). The wide-angle diffraction is diffuse ($d=0.45$ nm) and forms a ring with a maximum on the meridian, as also observed for the high-temperature mesophase of the isomeric linear compound **Lin22**. The mesophase grows with a characteristic shape and finally forms a mosaic texture (Figure 10). This texture is often seen for smectic phases



Figure 10. Texture of compound **Bra22** as seen for the Lam_Sm -phase during the growing of the mesophase (crossed polarizers; dark areas are residues of the isotropic liquid phase) at $T=105^\circ\text{C}$.

with additional in-plane order and also for columnar mesophases. As no in-plane periodicity can be detected by means of X-ray scattering, it is likely that this mesophase is a Lam_Sm phase with a 1D periodicity in the aromatic sublayers, but only a short- or medium-range positional correlation between the layers, the same as already discussed for the high-temperature mesophase of compound **Lin22** with a linear chain (Lam_Sm). However, the giant $\text{Col}_{\text{rec}(6)\text{cyl-8}}/c2mm$ cylinder phase, seen as a low temperature phase below the Lam_Sm phase for compound **Lin22** with a linear chain, is not observed in the branched compound **Bra22** with the same size of the lateral substituent. The reason for the loss of this

cylinder structure in the case of **Bra22** might be that the branching is located close to the biphenyl core. This increases the area required by the lateral groups at the aromatic–aliphatic interfaces and therefore it becomes more difficult to curve these interfaces as required for the formation of polygonal cylinders. This indicates that beside the overall space required by the lateral group also their distinct shape influences the mesophase morphologies. Comparison of compounds **Lin22**, **Ment***, and **Bra22**, all having the same volume fraction of the lateral groups of $f_{OR}=0.58$ (see Table 2) indicates that bulky groups at the end of the chains do not disturb the formation of cylinder structures and even stabilize these phases, whereas branching close to the aromatic core disfavors cylinder structures and favors the formation of Lam phases. Even bolaamphiphiles with much shorter branched chains form exclusively Lam-type phases as will be reported in detail in a subsequent manuscript.^[38]

Compounds with benzoate units in the lateral chain: A widely used building block for induction of LC properties in a broad variety of different compounds is based on mono-, di-, and trialkoxy-substituted benzoates.^[1,2,5,6,9,51] Herein, such benzoates were used as bulky end-groups, which were connected with the biphenyl core by means of hexyloxy or undecyloxy spacers (compounds **Benz6/m** and **Benz11/3**, respectively). Compounds **Benz6/1** and **Benz6/2** with only one or two dodecyloxy chains attached to the benzoate unit show monotropic mesophases whereas compounds **Benz6/3** and **Benz11/3** with three chains form enantiotropic phases (Table 2).

The mesophase of **Benz6/1** develops with a spherulitic texture (see Figure 11a) and only one layer reflection corresponding to $d=4.04$ nm was observed in the X-ray diffraction pattern (Figure S8). Based on texture and X-ray data it is assumed that this is a Lam_{Sm} phase, similar to that observed for the compounds **Lin22** and **Bra22**. The X-ray diffraction pattern of the monotropic mesophase of the dialkyl benzoate **Benz6/2** is very similar to that of **Benz6/1**, indicating a lamellar phase with $d=4.70$ nm (see Figure S9). However, the texture is quite distinct, characterized by a highly fluid schlieren-like appearance (see Figure 11b). Such textures are typically observed for Lam_N phases.^[18] In these Lam_N phases the bolaamphiphilic cores have only an orientational long-range order, but without periodicity in the aromatic layers (Figure 11b, right).^[18]

Compound **Benz6/3** behaves completely different and shows a hexagonal columnar phase as indicated by the texture (Figure 11c) and the X-ray diffraction pattern of an aligned sample (see Figure S10). The lattice parameter ($a_{hex}=4.95$ nm) is much larger than that allowed for a hexagonal honeycomb structure (expected value: $a_{hex}=3.5–3.6$ nm, according to $a_{hex}=3^{1/2}L$; $L=2.1$ nm) and, hence, this hexagonal columnar phase should be quite distinct from the honeycomb like cylinder structures of the n -alkyl-substituted compounds **Lin n** (with $n=11–16$). In the Col_{hex} phase of **Benz6/3** the bolaamphiphilic cores should form the interior of the columns and the lateral chains are organized around

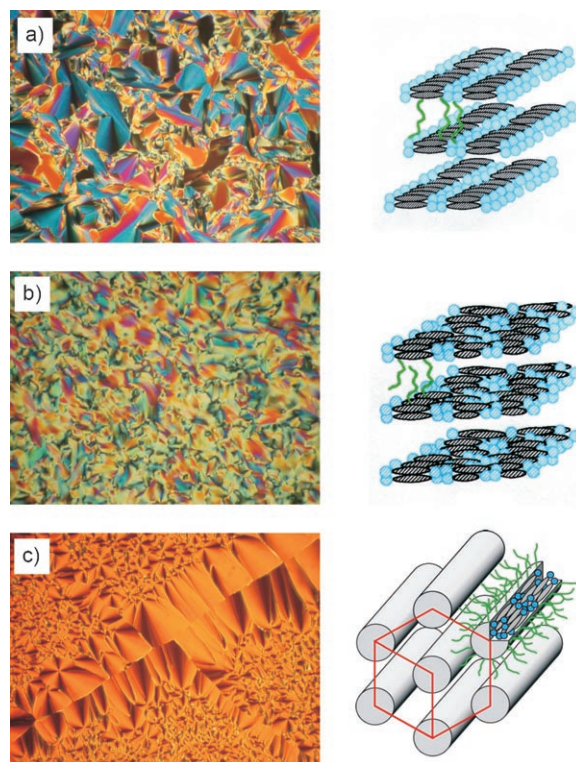


Figure 11. Textures of the mesophases of compounds **Benz6/m** as seen between crossed polarizers (left) and models of the organization of the molecules in the mesophases (right): a) Lam_{Sm} phase of **Benz6/1**; at 80°C; b) Lam_N phase of **Benz6/2** at 100°C; c) noncylinder Col_{hex} phase of **Benz6/3** at 115°C.

these columns forming a nonpolar continuum (see Figure 11c right). This phase structure is very similar to inverted Col_{hex} phases of simple amphiphilic molecules, but it is likely that the aromatic cores are aligned parallel to the column long axis.^[52] In this case the bolaamphiphilic structure of the polar groups can induce an additional (orientational and possibly also positional) order within these columns (similar to the organization in the layers of the Lam_N/Lam_{Sm} phases) as shown in Figure 11c at the right. If such a structure is assumed, approximately 12 molecules are organized in a hexagonal unit cell with a height of $h=1.8$ nm (corresponding to the shortest possible length of the bolaamphiphilic core with a compact conformation of the glycerol units^[53]), which means that about 12 biphenyl cores should form the cross section of the column cores.^[54]

Interestingly, elongation of the spacer unit from C_6 to C_{11} in compound **Benz11/3** restores the lamellar mesophase (X-ray diffraction pattern, see Figure S11), because the increased distance of the benzoate branching point from the biphenyl core decreases the overall taper angle of the lateral substituent and this reduces the curvature of the aromatic–aliphatic interface. The increased spacer length also allows a better intercalation of the three dodecyloxy chains with the aliphatic spacer units, which additionally contributes to a reduction of curvature. Hence, the lateral chains should be completely intercalated and strongly folded in this lamellar

phase. The texture of this lamellar phase is very similar to that observed for compound **Benz 6/2** (see Figure 11b), indicating a Lam_N phase. In contrast to the monotropic Lam_N phase of **Benz 6/2**, this mesophase is enantiotropic. No transition to a Lam_{Sm} phase is observed in the whole mesomorphic temperature range and this compound has the broadest Lam_N range ever achieved. Hence, these benzoates are ideal candidates for more detailed investigations of the Lam_N phases, for exploring their potential for applications and to access new phase structures.

Conclusion

A universal building block for the convergent synthesis of a wide variety of different T-shaped ternary amphiphiles with complex structures of the lateral chains was developed (compound **5**, see Schemes 1 and 2). As a consequence of this synthetic strategy, the T-shaped bolaamphiphiles obtained by etherification of **5** contain an additional ether linkage between aromatic core and lateral chain. The influence of this additional ether linkage on the mesomorphic properties was investigated for the *n*-alkyl-substituted compounds **Lin n**, and it turned out that fundamentally the same superstructures as previously reported for related *n*-alkyl-substituted compounds without ether oxygen can be found. However, these ether oxygen atoms reduce the flexibility of the connection between aromatic core and lateral chain and this restricts the packing of the lateral chains. Therefore, an increase of the melting points, a reduction of the mesophase stabilities, and a suppression of polygonal cylinder phases with relatively small cylinder cross sections is observed as a result of the introduction of the ether linkage. Also the unusual transition from a smaller 6-hexagon ($\text{Col}_{\text{hex}(6)\text{cyl-6}}/p6mm$ phase) to a larger 8-hexagon cylinder structure ($\text{Col}_{\text{rec}(6)\text{cyl-8}}/c2mm$ phase) by reducing the temperature can be explained by the better packing of less flexible chains in the giant cylinders. The fact that molecules with lateral alkoxy chains have reduced mesophase stabilities compared to alkyl derivatives is opposite to the trends usually seen for rodlike molecules with terminally attached chains.

As this synthetic strategy also allows an easy synthesis of compounds with much larger lateral groups, giant cylinder structures as well as Lam_N and Lam_{Sm} phases, reported previously only for fluorinated molecules,^[12b] became available also for non-fluorinated T-shaped bolaamphiphiles.

Polygonal cylinder arrays composed of 6-hexagons and giant 8-hexagons were also obtained for compounds in which additional bulky groups were attached to the ends of the lateral chain, which in the future will allow the introduction of functionality into these cylinders. The largest lateral

groups were obtained by attaching bis- and tris-(alkoxy)benzoate groups to the lateral chains. With these molecules broad regions of Lam_N phases and new noncylinder hexagonal columnar phases were realized.

The complete phase sequence observed for the series of new compounds is shown in Figure 12. Though some of the ternary amphiphiles have very large lipophilic parts, their mesophase behavior is still influenced by the bolaamphiphil-

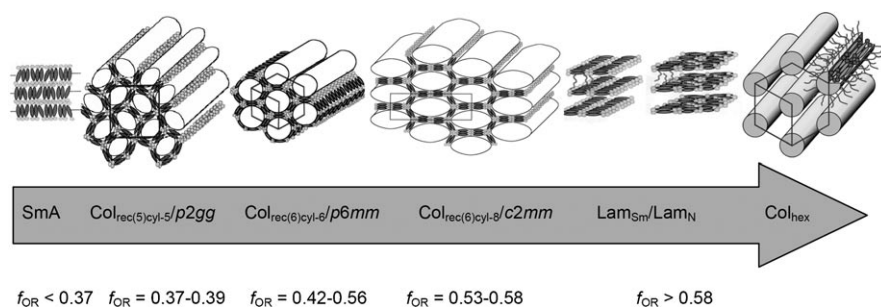


Figure 12. Phase sequence of T-shaped bolaamphiphiles, reported herein, as observed by enlarging the size of the lateral group.

ic structure of the polar group and these molecules behave like T-shaped ternary amphiphiles rather than as simple flexible binary amphiphiles.

Though the mesophase morphology is largely determined by the volume of the lateral chains with respect to the length of the rodlike building blocks, changes of other molecular parameters have a significant impact on molecular self-assembly. For example, bulky substituents located at the end of the lateral chain are compatible with the polygonal cylinder structures, whereas the cylinders are removed by branching the chains close to the connection with the aromatic core. This leads to a dominance of Lam_{Sm} phases also for molecules with smaller volume fractions of the lateral groups.^[38]

Compounds **Chol*n** with laterally attached cholesteryl groups show a remarkable new type of lamellar phases, in which two different types of layers with a distinct orientation of the rodlike units with respect to the layer planes are combined in a common mesophase. This shows that the relatively simple mode of self-organization in layers has still many unexplored possibilities and additional new structures could be expected by further increasing the molecular complexity by tailoring the shape, topology, and incompatibility of the building blocks.

In summary, these investigations have shown that T-shaped ternary amphiphiles are successful materials for the design of soft-matter systems with complex superstructures and that this structural information is quite robust, so that it can even dominate the self-assembly of molecules with quite large lateral groups. This will be used in future work for the design of functional soft matter materials based on these ternary amphiphiles.

Experimental Section

Investigations: All compounds with exception of the higher homologues were hygroscopic materials which take up humidity from air. This influenced the stability of LC phases and higher water concentrations could also lead to a change of the phase type.^[55] This required that all experiments were carried out with dried samples under exclusion of humidity. This was usually achieved by heating the samples on the glass substrate (for polarizing microscopy) or in the open DSC pan (for DSC) to 150 °C for about 10 s. These samples were immediately sealed and investigated. For X-ray experiments with aligned samples this strict exclusion of humidity was not possible, and therefore the results obtained by this method were cross-checked with diffraction patterns obtained from powder patterns in sealed capillaries.

Transition temperatures were measured by means of a Nikon Optiphot polarizing microscope with a Mettler FP82HT hot stage and control unit and confirmed using differential scanning calorimetry (DSC-7, Perkin-Elmer). The heating and cooling rates were 10 K min⁻¹.

Powder X-ray investigations were carried out with a Guinier film camera (Huber), samples in glass capillaries (∅ 1 mm) in a temperature-controlled heating stage, quartz-monochromatized Cu_{Kα} radiation, 30 to 60 min exposure time, calibration with the powder pattern of Pb(NO₃)₂. Aligned samples were obtained on a glass plate. Alignment was achieved upon slow cooling (rate: 1 K min⁻¹–0.01 K min⁻¹) of a small droplet of the sample and took place at the sample–glass or at the sample–air interface, with domains fiberlike disordered around an axis perpendicular to the interface. The aligned samples were held on a temperature-controlled heating stage and the diffraction patterns were recorded with a 2D detector (HI-STAR, Siemens, X-ray beam parallel to the substrate surface).

Synthesis and analytical data: Unless otherwise noted, all starting materials were purchased from commercial sources and were used as obtained. Preparative thin-layer chromatography was performed with a Chromatron (Harrison-Research) using silica gel 60 PF₂₅₄ (Merck). Column chromatography was performed with silica gel 60 (63–200 μm, Merck). For **Lin 18** the synthesis is described as an example; the synthesis of all other compounds was done in an analogous way. For compounds **Lin n** analytical data are given in the Supporting Information and for all other intermediates and end-compounds the procedures and analytical data are described in the Supporting Information.

1-Allyloxy-2-benzyloxy-4-bromophenol: A mixture of compound **2**^[23] (38.9 g, 0.14 mol), allyl bromide (18.5 g, 0.15 mol) and K₂CO₃ (96.3 g, 0.70 mol) in acetonitrile (500 mL) was stirred for 6 h under reflux. After cooling to room temperature, the reaction mixture was poured into an ice/water mixture (500 mL) and extracted with diethyl ether (3 × 100 mL). The combined organic layers were washed with water and brine. After drying over anhydrous Na₂SO₄, filtration and evaporation of the solvent, the crude product was purified by crystallization from methanol. Colorless solid; yield: 40 g (90%); m.p. 50–52 °C; ¹H NMR (400 MHz, CDCl₃, 25 °C, TMS): δ = 7.42 (d, ³J(H,H) = 6.8 Hz, 2H; Ar-H), 7.36 (t, ³J(H,H) = 7.3 Hz, 2H; Ar-H), 7.30 (d, ³J(H,H) = 7.1 Hz, 1H; Ar-H), 7.04 (d, ⁴J(H,H) = 2.3 Hz, 1H; Ar-H), 7.00 (dd, ³J(H,H) = 8.6 Hz, ⁴J(H,H) = 2.3 Hz, 1H; Ar-H), 6.76 (d, ³J(H,H) = 8.6 Hz, 1H; Ar-H), 6.08–5.99 (m, 1H; CH=CH₂), 5.38 (dd, ³J(H,H) = 17.3 Hz, ²J(H,H) = 1.6 Hz, 1H; CH=CH₂), 5.26 (dd, ³J(H,H) = 10.5 Hz, ²J(H,H) = 1.4 Hz, 1H; CH=CH₂), 5.09 (s, 2H; OCH₂Ph), 4.57 ppm (dt, ³J(H,H) = 5.2 Hz, ⁴J(H,H) = 1.6 Hz, 2H; OCH₂).

3-(2-Benzyloxy-4-bromophenoxy)propane-1,2-diol: To a mixture of 1-allyloxy-2-benzyloxy-4-bromophenol (20 g, 62.7 mmol) in acetone (150 mL) was added *N*-methylmorpholine-*N*-oxide (8 g, 68.9 mmol of a 50 wt % aq. solution) and OsO₄ (2 mL of a 0.004 M solution in *tert*-butanol). The mixture was stirred at room temperature for 48 h. After addition of saturated Na₂SO₃ solution in water (50 mL), the mixture was stirred for 30 min. Then, the solution was filtered through silica gel and the solvent was removed under reduced pressure. The residue was taken up in EtOAc (100 mL) and the aqueous layer was extracted with EtOAc (3 × 50 mL). The combined organic layers were washed with 10% aq. H₂SO₄, sat. aq. NaHCO₃, water, and brine. After drying over anhydrous Na₂SO₄, filtra-

tion and evaporation of the solvent, the crude product was crystallized from hexane/EtOAc (3:1, v/v). Colorless solid; yield: 20.7 g (93%); m.p. 112–114 °C; ¹H NMR (400 MHz, [D₆]acetone, 25 °C, TMS): δ = 7.50 (d, ³J(H,H) = 6.8 Hz, 2H; Ar-H), 7.38 (t, ³J(H,H) = 7.3 Hz, 2H; Ar-H), 7.31 (d, ³J(H,H) = 7.3 Hz, 1H; Ar-H), 7.17 (d, ⁴J(H,H) = 2.3 Hz, 1H; Ar-H), 7.06 (dd, ³J(H,H) = 8.6 Hz, ⁴J(H,H) = 2.3 Hz, 1H; Ar-H), 6.97 (d, ³J(H,H) = 8.6 Hz, 1H; Ar-H), 5.16 (s, 2H; OCH₂Ph), 4.12–4.08 (m, 1H; CHOH), 4.04–3.96 (m, 2H; CH₂OH), 3.74–3.59 ppm (m, 2H; OCH₂).

4-(2-Benzyloxy-4-bromophenoxy)-2,2-dimethyl-1,3-dioxolane (3): A suspension of 3-(2-benzyloxy-4-bromophenoxy)propane-1,2-diol (20.7 g, 58.6 mmol) and pyridinium *p*-toluenesulfonate (0.05 g, 0.2 mmol) in 2,2-dimethoxypropane (400 mL) was stirred at room temperature for 24 h. Thereafter, the solvent was evaporated and the residue was taken up in diethyl ether. The solution was washed with sat. aq. NaHCO₃, water, and brine. After drying over anhydrous Na₂SO₄, the solvent was removed under reduced pressure and the crude product was purified by column chromatography (silica gel, chloroform/methanol, 10:0.2, v/v). Colorless solid; yield: 22.3 g (97%); m.p. 66–68 °C; ¹H NMR (400 MHz, CDCl₃, 25 °C, TMS): δ = 7.41 (d, ³J(H,H) = 6.7 Hz, 2H; Ar-H), 7.36 (t, ³J(H,H) = 7.2 Hz, 2H; Ar-H), 7.31 (d, ³J(H,H) = 7.0 Hz, 1H; Ar-H), 7.05 (d, ⁴J(H,H) = 2.3 Hz, 1H; Ar-H), 7.01 (dd, ³J(H,H) = 8.5 Hz, ⁴J(H,H) = 2.3 Hz, 1H; Ar-H), 6.80 (d, ³J(H,H) = 8.5 Hz, 1H; Ar-H), 5.05 (s, 2H; OCH₂Ph), 4.46–4.40 (m, 1H; OCH), 4.11–4.05 (m, 2H; OCH₂), 3.97–3.90 (m, 2H; OCH₂), 1.40 (m, 3H; CH₃), 1.37 ppm (s, 3H; CH₃).

3-Benzyloxy-4,4'-bis(2,2-dimethyl-1,3-dioxolane-4-ylmethoxy)biphenyl: A mixture of **3** (11 g, 28 mmol), **4**^[12a] (8.46 g, 33.6 mmol), [Pd(PPh₃)₄] (1.62 g, 1.4 mmol), glyme (100 mL), and sat. aq. NaHCO₃ (75 mL) was stirred under an argon atmosphere at reflux for 12 h. After cooling to room temperature, the solvent was removed and the residue was extracted with chloroform (3 × 50 mL). The combined organic layers were washed with water and brine. After drying over anhydrous Na₂SO₄, the solvent was removed under reduced pressure, and the residue was taken up in chloroform and filtered through a plug of silica gel. After evaporation of the solvent the crude product was crystallized from chloroform/petroleum ether (1:1, v/v). Colorless solid; yield: 8.4 g (58%); m.p. 93–95 °C; ¹H NMR (400 MHz, CDCl₃, 25 °C, TMS): δ = 7.45–7.28 (m, 5H; Ar-H), 7.11 (d, ⁴J(H,H) = 1.9 Hz, 1H; Ar-H), 7.07 (dd, ³J(H,H) = 8.2 Hz, ⁴J(H,H) = 2.1 Hz, 1H; Ar-H), 5.14 (s, 2H; OCH₂Ph), 4.48 (quint, ³J(H,H) = 6.1 Hz, 2H; OCH), 4.18–4.06 (m, 4H; OCH₂), 4.03–3.88 (m, 4H; OCH₂), 1.46 (s, 3H; CH₃), 1.42 (s, 3H; CH₃), 1.40 (s, 3H; CH₃), 1.38 ppm (s, 3H; CH₃).

4,4'-Bis(2,2-dimethyl-1,3-dioxolane-4-ylmethoxy)biphenyl-3-ol (5): 2,2-Dimethyl-4-[2-benzyloxy-4'-(2,2-dimethyl-1,3-dioxolane-4-ylmethoxy)biphenyl-1,3-dioxolane (1.5 g, 2.88 mmol) was dissolved in THF (50 mL). Under an argon atmosphere Pd/C (0.03 g; 10% Pd) was added and the reaction mixture was flushed with hydrogen. After shaking this mixture at 40 °C and 2.8 bar hydrogen pressure for 12 h the catalyst was filtered off and the solvent was evaporated. The crude product was purified by crystallization from EtOAc/petroleum ether (1:1, v/v). Colorless solid; yield: 1.1 g (89%); m.p. 135–137 °C; ¹H NMR (400 MHz, CDCl₃, 25 °C, TMS): δ = 7.44 (d, ³J(H,H) = 8.9 Hz, 2H; Ar-H), 7.13 (d, ⁴J(H,H) = 2.2 Hz, 1H; Ar-H), 6.98 (dd, ³J(H,H) = 8.3 Hz, ⁴J(H,H) = 2.2 Hz, 1H; Ar-H), 6.94 (d, ³J(H,H) = 8.8 Hz, 2H; Ar-H), 6.92 (d, ³J(H,H) = 8.4 Hz, 2H; Ar-H), 6.24 (brs, 1H; OH), 4.48 (quint, ³J(H,H) = 5.8 Hz, 2H; OCH), 4.18–4.03 (m, 4H; OCH₂), 3.97–3.88 (m, 4H; OCH₂), 1.49 (s, 3H; CH₃), 1.46 (s, 3H; CH₃), 1.41 (s, 3H; CH₃), 1.40 ppm (s, 3H; CH₃).

4,4'-Bis(2,2-dimethyl-1,3-dioxolane-4-ylmethoxy)-3-octadecyloxybiphenyl (6): A mixture of **5** (150 mg, 0.35 mmol), 1-bromooctadecan (134 mg, 0.37 mmol), K₂CO₃ (242 mg, 1.75 mmol), and tetrabutylammonium iodide (5 mg) in anhydrous DMF (50 mL) was stirred at 80 °C for 6 h. After cooling to room temperature, the reaction mixture was poured into ice-water (50 mL), and the aqueous layer was extracted with diethyl ether (3 × 50 mL). The combined organic layers were washed with sat. aq. LiCl, water, and brine. After drying over anhydrous Na₂SO₄, filtration and evaporation of the solvent, the crude product was purified by preparative thin-layer chromatography (silica gel, petroleum ether/chloroform, 1:2, v/v). Colorless solid; yield: 160 mg (67%); m.p. 37–39 °C; ¹H NMR (200 MHz, CDCl₃, 25 °C, TMS): δ = 7.44 (d, ³J(H,H) = 8.9 Hz, 2H; Ar-H),

7.04–7.00 (m, 2H; Ar-H), 6.94 (d, $^3J(\text{H,H})=8.8$ Hz, 3H; Ar-H), 4.48 (quint, $^3J(\text{H,H})=5.9$ Hz, 2H; OCH), 4.20–3.86 (m, 10H; OCH₂), 1.81 (quint, $^3J(\text{H,H})=6.9$ Hz, 2H; OCH₂CH₂), 1.46 (m, 6H; CH₃), 1.39 (s, 6H; CH₃), 1.33–1.22 (m, 30H; CH₂), 0.86 ppm (t, $^3J(\text{H,H})=6.4$ Hz, 3H; CH₃).

3-[4'-(2,3-Dihydroxypropoxy)-3-octadecyloxybiphenyl-4-yloxy]propane-1,2-diol (Lin 18): A mixture of **6** (160 mg, 0.23 mmol) and 10% HCl (5 mL) in MeOH (20 mL) was heated to reflux for 3 h. The progress of the reaction was monitored by TLC. The solvent was evaporated and sat. aq. NaHCO₃ (20 mL) was added to the resulting mixture to obtain a precipitate. The precipitate was filtered off and washed with water and petroleum ether. The crude product was purified by repeated crystallization from methanol. Colorless solid; yield: 120 mg (85%); ¹H NMR (400 MHz, [D₅]pyridine, 25 °C, TMS): $\delta=7.68$ (d, $^3J(\text{H,H})=8.8$ Hz, 2H; Ar-H), 7.40 (s, 1H; Ar-H), 7.25 (s, 2H; Ar-H), 7.21–7.19 (m, 2H; Ar-H, overlapped by pyridine), 4.64–4.44 (m, 6H; OCH, OCH₂), 4.30–4.22 (m, 4H; OCH₂), 4.12 (t, $^3J(\text{H,H})=6.5$ Hz, 2H, OCH₂CH₂), 1.81 (quint, $^3J(\text{H,H})=7.1$ Hz, 2H, OCH₂CH₂), 1.50–1.47 (m, 2H; CH₂), 1.28–1.25 (m, 28H; CH₂), 0.85 ppm (t, $^3J(\text{H,H})=6.8$ Hz, 3H; CH₃); ¹³C NMR (100 MHz, [D₅]pyridine, 25 °C): $\delta=159.1, 150.2, 149.2, 134.8, 133.9, 128.2$ (2C), 119.6, 115.7, 115.5 (2C), 113.5, 72.6, 71.6 (2C), 71.2, 69.7, 64.7, 64.5, 32.3, 30.2 (4C), 30.2 (2C), 30.2, 30.1, 30.1 (2C), 30.1, 29.9, 29.8, 26.6, 23.1, 14.5 ppm; elemental analysis calcd (%) for C₃₆H₅₈O₇: C 71.72, H 9.70; found: C 71.80, H 9.89.

Acknowledgements

This work was supported by the government of Sachsen Anhalt through the Cluster of Excellence “Nanostructured Materials” and as part of the European Science Foundation EUROCORES Programme SONS, project SCALES by funds from the DFG and the EC Sixth Framework Programme, under contract No. ERAS-CT-2003-989409.

- [1] *Handbook of Liquid Crystals, Vol. 1–3* (Eds.: D. Demus, J. W. Goodby, G. W. Gray, H.-W. Spiess, V. Vill), Wiley-VCH, Weinheim, 1998.
- [2] a) C. Tschierske, *Annu. Rep. Prog. Chem. Sect. C* **2001**, *97*, 191–268; b) J. W. Goodby, G. H. Mehl, I. M. Saez, R. P. Tuffin, G. Mackenzie, R. Auzély-Velty, T. Benvegnu, D. Plusquellec, *Chem. Commun.* **1998**, 2057–2070; c) B. Donnio, D. Guillon, *Adv. Polym. Sci.* **2006**, *201*, 45–155; d) T. Kato, N. Mizoshita, K. Kishimoto, *Angew. Chem.* **2006**, *118*, 44–74; *Angew. Chem.* **2006**, *45*, 38–68; e) M. Lee, B.-K. Cho, W.-C. Zin, *Chem. Rev.* **2001**, *101*, 3869–3892; f) I. M. Saez, J. W. Goodby, *J. Mater. Chem.* **2005**, *15*, 26–40; g) D. L. Gin, X. Lu, P. R. Nemade, C. S. Pecinovsky, Y. Xu, M. Zhou, *Adv. Funct. Mater.* **2006**, *16*, 865–878.
- [3] S. Förster, M. Konrad, *J. Mater. Chem.* **2003**, *13*, 2671–2688.
- [4] a) C. Tschierske, *J. Mater. Chem.* **1998**, *8*, 1485–1508; b) W. Chen, B. Wunderlich, *Macromol. Chem. Phys.* **1999**, *200*, 283–311; c) C. Tschierske, *J. Mater. Chem.* **2001**, *11*, 2647–2671; d) C. Tschierske, *Curr. Opin. Colloid Interface Sci.* **2002**, *7*, 69–80.
- [5] a) K. Borisch, S. Diele, P. Göring, H. Müller, C. Tschierske, *Liq. Cryst.* **1997**, *22*, 427–443; b) K. Borisch, S. Diele, P. Göring, H. Kresse, C. Tschierske, *J. Mater. Chem.* **1998**, *8*, 529–543.
- [6] U. Stebani, G. Lattermann, R. Festag, M. Wittenberg, J. H. Wendorff, *J. Mater. Chem.* **1995**, *5*, 2247–2251.
- [7] I. W. Hamley, *The Physics of Block-Copolymers*; Oxford University Press, Oxford, **1998**, pp. 24–130.
- [8] a) J. M. Seddon, R. H. Templer in *Handbook of Biological Physics, Vol. 1* (Eds.: R. Lipowsky, E. Sackmann), Elsevier, Amsterdam, **1995**, pp. 97–160; b) S. Hassan, W. Rowe, G. J. T. Tiddy in *Handbook of Applied Surface and Colloid Chemistry, Vol. 1* (Ed.: K. Holmberg), Wiley, Chichester, **2002**, pp. 465–508.
- [9] a) G. Ungar, Y. Liu, X. Zeng, V. Percec, W.-D. Cho, *Science* **2003**, *299*, 1208–1211; b) X. Zeng, G. Ungar, Y. Liu, V. Percec, A. E. Dulcey, J. K. Hobbs, *Nature* **2004**, *428*, 157–160; c) V. Percec, C. M. Mitchell, W.-D. Cho, S. Uchida, M. Glodde, G. Ungar, X. Zeng, Y. Liu, V. S. K. Balagurusamy, P. A. Heiney, *J. Am. Chem. Soc.* **2004**, *126*, 6078–6094.
- [10] F.-G. Tournilhac, L. M. Blinov, J. Simon, S. V. Yablonsky, *Nature* **1992**, *359*, 621–623; S. Pencsek, F.-G. Tournilhac, P. Bassoul, C. Durlinat, *J. Phys. Chem. B* **1998**, *102*, 52–60.
- [11] C. Tschierske, *Chem. Soc. Rev.* **2007**, *36*, 1930–1970.
- [12] T-shaped bolaamphiphiles: a) M. Kölbl, T. Beyersdorff, X. H. Cheng, C. Tschierske, J. Kain, S. Diele, *J. Am. Chem. Soc.* **2001**, *123*, 6809–6818; b) X. H. Cheng, M. Prehm, M. K. Das, J. Kain, U. Baumeister, S. Diele, D. Leine, A. Blume, C. Tschierske, *J. Am. Chem. Soc.* **2003**, *125*, 10977–10996; c) X. H. Cheng, M. K. Das, U. Baumeister, S. Diele, C. Tschierske, *J. Am. Chem. Soc.* **2004**, *126*, 12930–12940; d) M. Prehm, F. Liu, U. Baumeister, X. Zeng, G. Ungar, C. Tschierske, *Angew. Chem.* **2007**, *119*, 8118–8121; *Angew. Chem. Int. Ed.* **2007**, *46*, 7972–7975; e) M. Prehm, G. Götz, P. Bäuerle, F. Liu, X. Zeng, G. Ungar, C. Tschierske, *Angew. Chem.* **2007**, *119*, 8002–8005; *Angew. Chem. Int. Ed.* **2007**, *46*, 7856–7859.
- [13] Correlated Lam phases: M. Prehm, S. Diele, M. K. Das, C. Tschierske, *J. Am. Chem. Soc.* **2003**, *125*, 614–615.
- [14] T-shaped facial amphiphiles: a) B. Chen, U. Baumeister, S. Diele, M. K. Das, X. Zeng, G. Ungar, C. Tschierske, *J. Am. Chem. Soc.* **2004**, *126*, 8608–8609; b) B. Chen, X. Zeng, U. Baumeister, S. Diele, G. Ungar, C. Tschierske, *Angew. Chem.* **2004**, *116*, 4721–4725; *Angew. Chem. Int. Ed.* **2004**, *43*, 4621–4625; *Angew. Chem. Int. Ed.* **2004**, *43*, 4621–4625; c) B. Chen, X. B. Zeng, U. Baumeister, G. Ungar and C. Tschierske, *Science* **2005**, *307*, 96–99; d) B. Chen, U. Baumeister, G. Pelzl, M. K. Das, X. B. Zeng, G. Ungar, C. Tschierske, *J. Am. Chem. Soc.* **2005**, *127*, 16578–16591; e) G. Cook, U. Baumeister, C. Tschierske, *J. Mater. Chem.* **2005**, *15*, 1708–1721; f) F. Liu, B. Chen, U. Baumeister, X. Zeng, G. Ungar, C. Tschierske, *J. Am. Chem. Soc.* **2007**, *129*, 9578–9579.
- [15] a) H.-A. Klok, S. Lecommandoux, *Adv. Mater.* **2001**, *13*, 1217–1229; b) O. Ikkala, G. ten Brinke, *Science* **2002**, *295*, 2407–2409.
- [16] a) F. S. Bates, G. H. Fredrickson, *Phys. Today* **1999**, 32–38; b) V. Abetz, P. F. W. Simon, *Adv. Polym. Sci.* **2005**, *189*, 125–212.
- [17] Y. Matsushita, *Macromolecules* **2007**, *40*, 771–776.
- [18] Lam phases: a) X. H. Cheng, M. K. Das, S. Diele, C. Tschierske, *Angew. Chem.* **2002**, *114*, 4203–4207; *Angew. Chem. Int. Ed.* **2002**, *41*, 4031–4035; b) M. Prehm, X. H. Cheng, S. Diele, M. K. Das, C. Tschierske, *J. Am. Chem. Soc.* **2002**, *124*, 12072–12073; c) N. M. Patel, M. R. Dodge, M. H. Zhu, R. G. Petschek, C. Rosenblatt, M. Prehm, C. Tschierske, *Phys. Rev. Lett.* **2004**, *92*, 015501; d) N. M. Patel, I. M. Syed, C. Rosenblatt, M. Prehm, C. Tschierske, *Liq. Cryst.* **2005**, *32*, 55–61.
- [19] This phase designation was introduced in reference [12c]; in the earlier references^[18a,b] Lam_{iso} was designated as SmA, Lam_N as SmA_N and Lam_{sm} as Lam_A (or Lam_X^[12b]).
- [20] a) N. Miyaura, T. Yanagi, A. Suzuki, *Synth. Commun.* **1981**, *11*, 513–519; b) M. Hird, G. W. Gray, K. J. Toyne, *Mol. Cryst. Liq. Cryst.* **1991**, *206*, 187–204; c) N. Miyaura, A. Suzuki, *Chem. Rev.* **1995**, *95*, 2457–2483.
- [21] J. H. Jones, G. T. Young, *J. Chem. Soc. C* **1968**, 436–441.
- [22] K. N. Edgar, S. N. Falling, *J. Org. Chem.* **1990**, *55*, 5287–5291.
- [23] Z. Xin, G. Liu, C. Abad-Zapatero, Z. Pei, B. G. Szczepankiewicz, X. Li, T. Zhang, C. W. Hutchins, P. J. Hajduk, S. J. Ballaron, M. A. Stashko, T. H. Lubben, J. M. Trevelyan, M. R. Jirousek, *Bioorg. Med. Chem. Lett.* **2003**, *13*, 3947–3950.
- [24] P. A. Grieco, M. Nishizawa, T. Oguri, S. D. Burke, N. Marinovic, *J. Am. Chem. Soc.* **1977**, *99*, 5773–5780.
- [25] V. Van Rheenen, D. Y. Cha, W. M. Hartley, *Org. Synth.* **1978**, *58*, 43–51.
- [26] C₆ to C₈/C₁₁ chains are relatively short chains for this type of mesogen, whereas for most classical mesogens these are usually regarded as chains of intermediate length or even as long chains.^[1]
- [27] Due to the monotropic character of the SmA phases of **Lin 6** and **Lin 8** and the rapid crystallization of the samples, the determination of *d* values by X-ray diffraction was not possible, but it is very likely that the organization of **Lin 6** and **Lin 8** in the SmA phases is identi-

- cal with the organization of the compounds **An** ($n=1-7$) in the enantiotropic SmA phases, which were investigated by X-ray scattering.^[12a] However, as no X-ray data were available, it is unclear if the SmA phases of **Lin 6** and **Lin 8** represent conventional SmA phases, characterized by sharp layer reflections or if they belong to the strongly distorted SmA⁺ type phases (as observed for compounds **An** with $n=3-7$, see Figure 2), for which a diffuse scattering is seen in the small-angle region. This diffuse scattering is attributed to the mean distance between the disordered microdomains containing the alkyl chains. The layer reflection is weak or completely absent, probably due to the low electron density modulation between the layers of the aromatic cores and the layers of the glycerol units.^[12a]
- [28] Bolaamphiphiles without lateral chains: F. Hentrich, C. Tschierske, H. Zschke, *Angew. Chem.* **1991**, *103*, 429–431; *Angew. Chem. Int. Ed. Engl.* **1991**, *30*, 440–441. F. Hentrich, S. Diele, C. Tschierske, *Liq. Cryst.* **1994**, *17*, 827–839; F. Hentrich, C. Tschierske, S. Diele, C. Sauer, *J. Mater. Chem.* **1994**, *4*, 1547–1558.
- [29] The superstructures reported herein represent ordered fluids, which means that there is a high degree of conformational, rotational, and translational mobility as indicated by the diffuse character of the wide-angle scattering seen by X-ray diffraction. Hence, these are highly dynamic fluid systems in which distinct regions with enhanced concentration of aromatic cores, regions of the polar hydrogen bonding groups, and regions of the nonpolar segments coexist in equilibrium structure with long-range periodicity.
- [30] A. Immirzi, B. Perini, *Acta Crystallogr. Sect. A* **1977**, *33*, 216–218.
- [31] As these cylinder structures represent dynamic (fluid) systems, the number of molecules in the cross section of the cylinder walls is an average number that does not necessarily represents an integer number; the cylinder walls can also be slightly thicker or thinner than exactly two molecules.
- [32] The structures of all types of cylinder phases reported herein were confirmed for representative examples of compounds **An** and their fluorinated analogues by electron density calculations based on synchrotron data: F. Liu, X. B. Zeng, X. Cheng, C. Tschierske, G. Ungar, unpublished results.
- [33] There is a small reduction of a_{hex} with increasing temperature. For example, for compound **An** with $n=18$ (**A18**^[12a]), the parameter a_{hex} is 3.65 nm at $T=80^\circ\text{C}$ and 3.60 nm at $T=130^\circ\text{C}$. The same tendency is found for the Col_{hex} phases of the compounds **Lin n**, but due to the smaller phase ranges of these compounds the change of the lattice parameter is much smaller and more difficult to measure accurately. In the case of classical columnar phases, in which the flexible alkyl chains form the shell around the column cores also a reduction of a_{hex} with increasing temperature was observed, but the temperature dependence is often much stronger. For example, in the case of star-shaped mesogens, a reduction of a_{hex} by 0.45 nm was observed for a temperature increase by 50 Kelvin (see: M. Lehmann, C. Köhn, H. Meier, S. Renker, A. Oehlhof, *J. Mater. Chem.* **2006**, *16*, 441–451). This means that increasing chain flexibility causes an expansion along the column long axis and leads to a shrinkage of the column diameter. In the case of the polygonal cylinder phases the polygonal frame not only restricts the expansion of the cylinders, it also limits the shrinkage of the cylinders and therefore the temperature dependence of the lattice parameters is in this case relatively small.
- [34] Remarkably, the volume of the lateral chains required for the transition from a hexagonal honeycomb to a stretched hexagonal honeycomb is identical for the series of bolaamphiphiles with fluorinated lateral chains (compounds of type **An**, see Figure 2, with $R=-(\text{CH}_2)_2\text{C}_{10}\text{F}_{21}$ instead of the $\text{C}_n\text{H}_{2n+1}$ chain; $V=0.453\text{ nm}^3$)^[12b] and compounds **Lin n** with simple alkyl chains (**Lin 18**; $V=0.453\text{ nm}^3$; if the ether oxygen is included for the calculation ($-\text{OC}_{18}\text{H}_{37}$ chain) a volume of $V=0.462\text{ nm}^3$ results, indicating that the ratio of the volume required by the lateral chains with respect to the surface area of the cylinder shells is the dominating effect that determines the mesophase morphology in this class of compounds.
- [35] The cubic expansion coefficients are $\alpha=81\times 10^{-5}\text{ K}^{-1}$ for dodecane and $\alpha=50\times 10^{-5}\text{ K}^{-1}$ for glycerol: D. R. Lide, H. V. Kehiaian, *CRC Handbook of Thermophysical and Thermochemical Data*, CRC, Boca Raton, **1994**; D. R. Lide, *Handbook of Chemistry and Physics*, CRC, Boca Raton, **1994**.
- [36] Interestingly, similar arguments were used to understand the temperature dependence of phase transitions in columnar phases formed by polycatenar molecules. The columnar phases of these compounds are reversed to the polygonal cylinder structures, as the rodlike cores are organized in the interior of the columns and the alkyl chains form a honeycomb-like isotropic continuum. In these systems the Col_{hex} phases at high temperature were often replaced by rectangular columnar phases at lower temperature. It was proposed that this phase transition is driven by reduction of chain mobility by reducing temperature, which is not isotropic and prohibits the formation of aromatic column cores with a circular cross section and hence, the symmetry is reduced: B. Donnio, B. Heinrich, H. Al-louchi, J. Kain, S. Diele, D. Guillon, D. W. Bruce, *J. Am. Chem. Soc.* **2004**, *126*, 15258–15268.
- [37] As mentioned in reference [33], with increasing temperature there is a reduction of the lateral expansion of the alkyl chains, which is compensated by additional expansion along the column long axis. This can also contribute to the stabilization of 6-hexagon cylinders at higher temperature.
- [38] M. Prehm, X. Cheng, C. Enders, S. Diele, M. K. Das, U. Baumeister, F. Liu, X. Zeng, G. Ungar, C. Tschierske, unpublished results.
- [39] The small electron density difference between aromatic cores and glycerol units can also be seen in some electron density maps obtained for the polygonal cylinder phases.^[12d]
- [40] Though the lateral ether oxygen atom has a low mobility and can be considered as a part of the rigid core it contributes to the space filling inside the cylinder frames.
- [41] H. J. Deutscher, R. Frach, C. Tschierske, H. Zschke in *Selected Topics in Liquid Crystal Research* (Ed.: H. D. Koswig), Akademie Verlag, Berlin, **1990**, pp. 1–18; E. Kleinpeter, H. Köhler, A. Lunow, C. Tschierske, H. Zschke, *Tetrahedron* **1988**, *44*, 1609–1612.
- [42] Z. Chen, V. Stepanenko, V. Dehm, P. Prins, L. D. A. Siebbeles, J. Seibt, P. Marquet, V. Engel, F. Würthner, *Chem. Eur. J.* **2007**, *13*, 436–449.
- [43] V. Percec, M. Glodde, T. K. Bera, Y. Miura, I. Shiyonovskaya, K. D. Singer, V. S. K. Balagurusamy, P. A. Heiney, I. Schnell, A. Rapp, H.-W. Spiess, S. D. Hudsonk, H. Duank, *Nature* **2002**, *419*, 384–387.
- [44] Though these stereogenic centers in the side chain are homogeneously chiral, due to the presence of the racemic stereogenic centers in the glycerol groups, the investigated systems actually represent mixtures of four distinct diastereomers.
- [45] H.-S. Kitzerow, C. Bahr, *Chirality in Liquid Crystals*, Springer, New York, **2001**.
- [46] R. Zentel, M. Brehmer, *Acta Polym.* **1996**, *47*, 141–149.
- [47] S. W. Cha, J. I. Jin, D.-C. Kim, W.-C. Zin, *Macromolecules* **2001**, *34*, 5342–5348.
- [48] W.-S. Bae, J.-W. Lee, J.-I. Jin, *Liq. Cryst.* **2001**, *28*, 59–67; J. Andersch, C. Tschierske, S. Diele, D. Lose, *J. Mater. Chem.* **1996**, *6*, 1297–1307; J.-W. Lee, X. L. Piao, Y.-K. Yun, J.-I. Jin, Y.-S. Kang, W.-C. Zin, *Liq. Cryst.* **1999**, *26*, 1671–1685.
- [49] Examples of linear oligomesogens: C. T. Imrie, P. A. Henderson, *Curr. Opin. Colloid Interf. Sci.* **2002**, *7*, 298–311; C. V. Yelamaggad, G. Shanker, *Liq. Cryst.* **2007**, *34*, 799–809; C. V. Yelamaggad, N. L. Bonde, A. S. Achalkumar, D. S. S. Rao, S. K. Prasad, A. K. Prajapati, *Chem. Mater.* **2007**, *19*, 2463–2472.
- [50] For shape amphiphiles composed of incompatible disc- and rodlike units see: R. W. Date, D. W. Bruce, *J. Am. Chem. Soc.* **2003**, *125*, 9012–9013.
- [51] C. Tschierske, *Prog. Polym. Sci.* **1996**, *21*, 775–852; U. Beginn, *Prog. Polym. Sci.* **2003**, *28*, 1049–1105.
- [52] A related structure with aromatic cores parallel to the column long axis was postulated for a polycatenar dithiolium salt: F. Artzner, M. Veber, M. Clerc, A. M. Levelut, *Liq. Cryst.* **1997**, *23*, 27–33.
- [53] Generally, in correlated Lam_{sm} phases the in-plane periodicity is around 1.8 nm for biphenyl derived bolaamphiphiles,^[13] corresponding to the shortest possible length of the bolaamphiphilic core with

most compact glycerol units, whereas in the polygonal cylinder phases the molecules adopt the most extended conformation with stretched glycerol units which leads to a length of $L = 2.1$ nm.^[11,12a,b] We assume that also in the Col_{hex} phase of **Benz3/6** the glycerol groups adopt a compact conformation as in the Lam phases.

[54] More detailed studies on this type of Col_{hex} phases in a series of structurally different bolaamphiphiles confirmed an arrangement of the rodlike cores parallel to the column long axis: M. Prehm, U. Baumeister, F. Liu, X. Zeng, G. Ungar, C. Tschierske, unpublished results.

[55] J. A. Schröter, C. Tschierske, M. Wittenberg, J. H. Wendorff, *J. Am. Chem. Soc.* **1998**, *120*, 10669–10675; R. Plehnert, J. A. Schröter, C. Tschierske, *J. Mater. Chem.* **1998**, *8*, 2611–2626; J. A. Schröter, C. Tschierske, M. Wittenberg, J. H. Wendorff, *Angew. Chem.* **1997**, *109*, 1160–1163; *Angew. Chem. Int. Ed. Engl.* **1997**, *36*, 1119–1121.

Received: January 23, 2008
Published online: June 2, 2008